Nuclear-spin-lattice relaxation rate of planar oxygen in $YBa_2Cu_3O_{6.52}$ and $YBa_{1.92}Sr_{0.08}Cu_3O_7$ single crystals

M. Horvatić,* C. Berthier, Y. Berthier, P. Ségransan, P. Butaud, W. G. Clark,† and J. A. Gillet
Laboratoire de Spectrométrie Physique, Université Joseph Fourier Grenoble I, Boîte Postale 87, 38402 Saint-Martin d'Hères, France

J. Y. Henry
Département de Recherche Fondamentale du Centre d'Etudes Nucléaires de Grenoble, 85X, 38041 Grenoble Cedex, France

(Received 28 December 1992; revised manuscript received 29 June 1993)

A full account is given of an NMR investigation of planar oxygen in the normal state ($T > T_c$) of two characteristic superconducting Y-Ba-Cu-O single crystals: $YBa_2Cu_3O_{6.52}$ representing the underdoped "60-K phase," and $YBa_{1.92}Sr_{0.08}Cu_3O_7$ representing the overdoped "90-K phase." (We argue that Sr impurities in the latter crystal do not significantly change the behavior of the system.) Data are analyzed within the framework of the Mila-Rice spin Hamiltonian and using inelastic-neutron-scattering results, in order to obtain detailed and consistent information on the antiferromagnetic fluctuations (AFF) in this system. Within the model, the filtering of the AFF at the oxygen site is always found to be imperfect, even for the AFF that are localized to a maximum degree in the $\mathbf{q}$ space around $\mathbf{Q}_{AF}$. In our overdoped sample this is also confirmed experimentally, in contradiction to other published data. Any shape of $\chi''(\mathbf{q}-\mathbf{Q}_{AF})$ that falls off slower than Gaussian is found to be incompatible with experimental data. In the underdoped regime, the observed temperature dependence of the T_1 anisotropy is in clear contradiction with any single-component model. A possible explanation could involve an extra contribution to relaxation coming from spinless quasiparticles.

I. INTRODUCTION

In the investigation of the electronic and magnetic structure of high-T_c superconducting oxides, NMR has brought a number of foundation stones that put severe constraints on any comprehensive microscopic theory of these fascinating materials.[1] Among the various compounds of this family, the $YBa_2Cu_3O_{6+x}$ system (YBCO) has been one of the most studied by this technique. On one hand, by varying the oxygen stoichiometry x between 0 and 1, it offers the possibility of describing a wide range in the phase diagram: antiferromagnetism for $x < 0.4$ and the metallic regime with low- and high-hole-doping level for x increasing from 0.4 to 1. On the other hand, through ^{63}Cu, ^{17}O, and ^{89}Y NMR, it offers a convenient opportunity to study the low-energy excitations in the CuO_2-Y-CuO_2 sandwich at different sites involving different wave functions and different symmetries.

As far as the normal state is concerned, several features are now well established by NMR.

(i) The quasilocalized character of the Cu(2) electronic spin,[2-4] which interacts with its two nearest-neighbor oxygen atoms O(2) and O(3) through a transferred hyperfine field,[5] a situation which is summarized in the so-called Mila-Rice spin Hamiltonian.[6]

(ii) From the comparison between the temperature dependence of $(T_1T)^{-1}$ for the Cu(2) and O(2,3) sites, it was possible quite early to infer the existence of antiferromagnetic fluctuations (AFF) in the normal state of these superconducting oxides,[7-9] the contribution of these AFF being filtered at the oxygen site due to a geometrical form factor.[10]

(iii) The possibility, as far as low-energy excitations are concerned, to reduce the starting three-band Hamiltonian to a single effective band approximation (like the t-J model[11]) has been demonstrated by comparing the temperature dependences of the axial and the isotropic part of the magnetic hyperfine shift (MHS) tensor of the O(2,3) site[8,9] in the substoichiometric $YBa_2Cu_3O_{6+x}$ ($x < 0.9$). The experimental results exclude the existence of an independent spin degree of freedom at the oxygen; at least, the contribution of such an additional spin susceptibility to the MHS is not larger than the error bars on the orbital part of the MHS.

(iv) The temperature dependence of the MHS tensor for the three nuclei at Cu(2),[12] O(2,3),[9,13,14] and Y[15] sites is the same as that of macroscopic susceptibility. From temperature independence of the apical oxygen O(4) MHS tensor, and the values of the MHS tensors of O(2,3) and Cu(2), it has been shown that the major part of the spin density is localized on the Cu(2) site, and that the temperature dependence of this spin susceptibility (χ^S) is mainly localized in the CuO_2 planes.[8,13] However, the microscopic origin of the temperature dependence of χ^S is not well understood on a theoretical basis yet.

(v) The nuclear-spin-lattice relaxation rate (NSLRR) divided by the temperature $(^{17}T_1T)^{-1}$ at the O(2,3) site has been found with a great accuracy to scale linearly with the MHS tensor $\mathbf{K}(T)$ (Refs. 9, 14, and 16) [$K(T)T_1T = \text{const}$], a behavior quite different from the well-known Korringa law ($K^2T_1T = \text{const}$) observed in the "traditional" three-dimensional metals. It seems

recognized now that $(^{89}T_1T)^{-1}$ at the yttrium site also obeys the same behavior, although the accuracy is much lower.[17]

(vi) Finally, it was shown by Horvatić *et al.*[2,3] that the temperature dependence of the Cu(2) NSLRR in $YBa_2Cu_3O_{6+x}$ could switch between two different behaviors: (a) For the so-called overdoped regime ($x>0.94$), $(^{63}T_1T)^{-1}$ continuously increases from high temperature down to T_c, followed by a sudden decrease just at the phase transition. In the normal state ($T>T_c$), the static spin susceptibility $\chi^S(T)$ remains constant (or rather slightly increasing[16,18,19]). (b) For underdoped samples ($x<0.94$), irrespective of the T_c value (90 or 60 K), the $(^{63}T_1T)^{-1}$ exhibits a maximum at a temperature T^* of the order of 130 K, which is well above T_c. In such a case, which is also the situation observed in $YBa_2Cu_4O_8$,[20] there is a strong decrease of $\chi^S(T>T_c)$ with decreasing temperature. The characteristic composition separating the two regimes ($x_c\cong 0.94$) corresponds to the maximum value of T_c observed "in the middle" of the so-called "90-K phase," so that two different magnetic behaviors can correspond to the same value of $T_c\cong 90$ K.

The temperature dependence of the NSLRR of the Cu(2), O(2,3), and Y sites has been consistently explained in the framework of the phenomenological model originally proposed by Millis, Monien, and Pines[21] (MMP) to explain the NMR results in $YBa_2Cu_3O_7$ and later modified to cover the $YBa_2Cu_3O_{6.65}$ (Ref. 22) as well. Using the Mila-Rice Hamiltonian and a random-phase-approximation (RPA) -like scheme to describe the dynamical spin susceptibility $\chi(\mathbf{q},\omega)=\chi'-i\chi''$, they managed to explain the temperature dependence of the various NSLRR's by combining the temperature dependence of the correlation length $\xi(T)$ of the AFF and that of the static susceptibility $\chi^S(T)$. These results have been reexamined in more detail in Ref. 23, where the authors concluded that their interpretation of NMR data is not consistent with susceptibilities deduced from inelastic neutron scattering[24–26] (INS). Indeed, the characteristic energy of the AFF ω_{SF} is predicted to be an order of magnitude lower than the values inferred from INS, as already discussed by Berthier *et al.*[27] The ξ values they obtained from NMR are significantly higher, however, we remark that in the lower limit of their Gaussian-fit estimate the INS values[24–26] are recovered. The analysis of the present article can be viewed as an investigation of this limiting case in an attempt to propose an analysis, which is consistent with neutron results. In order to ensure the consistency, the ξ values deduced from INS are taken to be the input parameters of the fit, and there are other important differences in the analysis and in the interpretation. The key point is the quantitative analysis of the cancellation of the AFF contribution to the oxygen O(2,3) NSLRR both in underdoped and overdoped regimes. The analysis is based on the accurate data on the O(2,3) MHS and NSLRR tensors obtained on well-defined $YBa_2Cu_3O_{6.52}$ and $YBa_{1.92}Sr_{0.08}Cu_3O_7$ single crystals (instead of oriented powders). Second, we focus on the NSLRR anisotropy for the O(2,3) site, as well as its temperature dependence. We compare the behavior in the overdoped sample, where the anisotropy is found to be temperature independent in the normal state,[16,28] to that in the underdoped sample, where it is temperature dependent.[16,29] The anisotropy of the oxygen NSLRR is shown to be a crucial test for any theoretical attempt to explain the NSLRR in the YBCO system. In particular, the temperature dependence of the anisotropy is not compatible with descriptions based only on the Mila-Rice (i.e., single component) Hamiltonian.

The paper is organized as follows: the next section is devoted to the samples, their characterization (with special attention paid to the discussion of Sr impurities in the $x=1$ sample), and to some experimental details. Section III presents the experimental results only, while the discussion and the interpretation of these results are given in the following two sections. In particular, the ^{17}O and ^{63}Cu NSLRR is discussed with respect to the neutron data and various MMP-like models in Sec. IV, while Sec. V is devoted to the analysis of the NSLRR anisotropy. The final section contains concluding remarks.

II. SAMPLES AND EXPERIMENT

Measurements presented in this paper have been carried out on two "porous" single crystals:[30] sample 1 on $YBa_{1.92}Sr_{0.08}Cu_3O_7$ and sample 2 on $YBa_2Cu_3O_{6.52}$, which were enriched in ^{17}O (typical size was $2\times1\times0.25$ mm^3). Details on the crystal preparation and characterization of porous crystals can be found in Ref. 30. As already discussed in Ref. 3, their main advantage, besides the size, is the more efficient oxygenation process, which is fundamental for the homogeneity of oxygen concentration in the samples. To enrich the crystals in ^{17}O, they were placed on an alumina nacelle inside a quartz tube in which the available volume for gas exchange was reduced to about 1 cm^3. After 3 h under vacuum, the quartz tube is filled with enriched oxygen (51% of ^{17}O) at a pressure of 0.8 bar, heated at 1193 K for 10 h, and cooled down to room temperature at a rate of 50 K/h. The gas left in the tube is replaced by enriched oxygen, the sample is heated again at 1193 K for 10 h, and then cooled down to 984 K, 793 K, and room temperature at cooling rate values of 20 K/h, 10 K/h, and 5 K/h, respectively. This last treatment allows us to reach a stoichiometry very close to $x=1$ for $YBa_2Cu_3O_{6+x}$. In order to obtain the stoichiometry $x=0.5$, a different procedure was applied: 200 mg of $YBa_2Cu_3O_{6.06}$ and $YBa_2Cu_3O_7$ ceramics already enriched in ^{17}O are mixed in equal quantities, placed into the alumina nacelle together with the ^{17}O enriched $YBa_2Cu_3O_7$ crystals (total weight of about 4 mg), and then sealed in the quartz tube with a very small available volume for gas. After heating at a rate of 300 K/h, the tube is maintained at 993 K for 10 h, and then cooled down to 793 K and room temperature at 10 K/h and 5 K/h cooling rates. The final stoichiometry was determined by measuring the weight change of the ceramics and found equal to $x=0.52\pm0.02$. The quality of samples is tested by the a.c. magnetic susceptibility measurements with weak alternating field applied along the *a-b* plane and results are shown in Fig. 1; the transition tem-

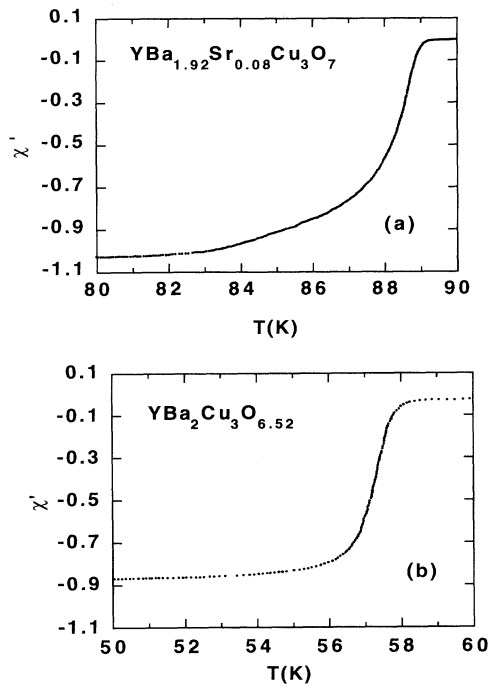

FIG. 1. Real part of the ac magnetic susceptibility $\chi'(T)-i\chi''(T)$ of (a) $YBa_{1.92}Sr_{0.08}Cu_3O_7$ (sample 1) and (b) $YBa_2Cu_3O_{6.52}$ (sample 2).

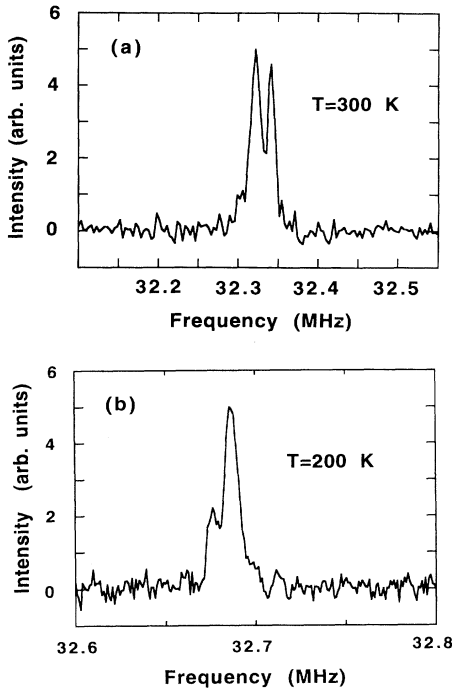

FIG. 2. Spectrum of the first low-frequency satellite [i.e., of transition (1/2,3/2)] of plane $^{17}O(2,3)$ in the $H_0\|Z$-axis configuration in (a) sample 1 and in (b) sample 2 (Z is parallel to the Cu—O—Cu bond).

peratures are found to be $T_c=89$ K and 59 K for samples 1 and 2, respectively.

Regarding sample 2, we note that despite its low oxygen content, the T_c is rather high; the same value is usually associated with $YBa_2Cu_3O_{6.67}$, where only $\frac{1}{3}$ of the chain oxygens O(1) are absent. We might speculate that properties of 60-K phase samples are rather dependent on the degree of ordering of oxygens in chains. With this respect, sample 2 can be regarded as being another well-ordered example of the 60-K phase, the one that is close to the case corresponding to emptying $\frac{1}{2}$ of the O(1) sites, instead of $\frac{1}{3}$ for the typical 60-K-phase oxygen concentration. This is supported by a very narrow superconducting transition shown in Fig. 1(b), as well as by rather narrow NMR lines as exemplified by Fig. 2(b) showing the oxygen (1/2,3/2) satellite line. Furthermore, as discussed in Refs. 2 and 28, the degree of order can be directly measured using the relative intensity of the "empty chain" $Cu(1,O_2)$ and the plane copper Cu(2) line. The experimental value of 0.45 ± 0.05 is considerably above the value 0.25, which is expected for a random distribution of oxygen vacancies and very close to the value 0.5, corresponding to perfect order.

According to the value of T_c, sample 1 clearly belongs to the 90-K phase; however, as the barium that was used in its synthesis contained 4% strontium, it is *a priori* not clear how the properties of this sample compare to the "pure" YBCO. For several reasons we argue that sample 1 is actually a very good representative of pure (overdoped) $YBa_2Cu_3O_7$ and that the only consequence of the presence of strontium (at least as far as the NMR results are concerned) is to slightly increase (over)doping, which is reflected in the corresponding decrease of T_c by $\cong 3$ K. First, although the width of NMR lines [which includes the width of the electric-field gradient (EFG) distribution] is very sensitive to impurities, all the NMR lines were found to be very narrow, and all the characteristic quantities [i.e., EFG, magnetic hyperfine shift (MHS) and NSLRR tensors] are equal or very close to results of other authors on high-quality $YBa_2Cu_3O_7$ samples. For example, in Fig. 2(a) the first satellite [i.e., (1/2,3/2) transition] of the O(2,3) spectrum is shown for the configuration when H_0 is parallel to the Cu-O-Cu bond, the so-called Z axis, where one can clearly distinguish the different contribution of O(2) and O(3) sites; the distributions of oxygen EFG are very narrow confirming the quality of the sample. Figure 3(a) shows that the temperature dependence of Cu(2) NSLRR compares very well to the published $YBa_2Cu_3O_7$ NMR data.[7] The anisotropy of Cu(2) relaxation $T_1^{-1}(\perp c)/T_1^{-1}(\|c)$ [Fig. 3(b)] is found to be temperature independent for $T>T_c$ and equal to 3.4 (except at $T=100$ K, where it reaches the value of 3.7) in agreement with recent data of Borsa *et al.*[31] but somewhat lower than 3.7 reported by Barrett *et al.*[32] [As an aside, we remark that in the determination of $T_1^{-1}(\perp c)$ NMR results one should take into account the corrections corresponding to perturbation of pure Zeeman spin states by the quadrupole Hamiltonian.[33]] Second, sample 1 is clearly overdoped as there is definitively *no trace* of

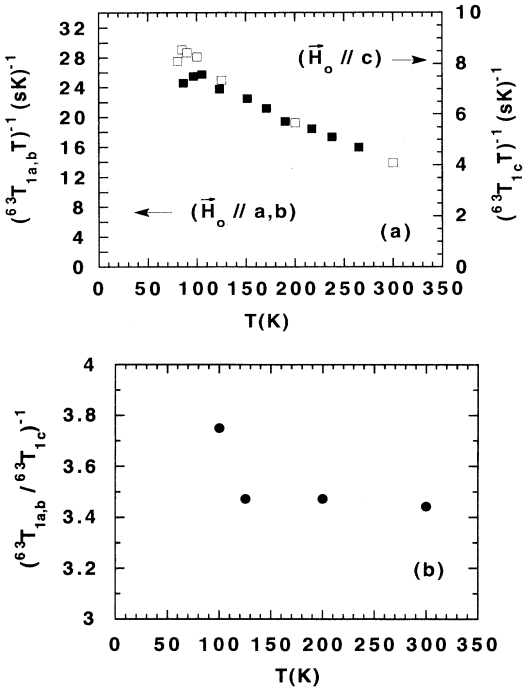

FIG. 3. (a) Normal state $(T_1T)^{-1}$ of planar copper Cu(2) in sample 1 ($\square, H_0 \| a$-b plane) compared to the ($\blacksquare, H_0 \| c$ axis) data reported by Hammel *et al.*[7] (b) NSLRR anisotropy (Ref. 33) $(T_{1_\perp}/T_{1_\parallel})^{-1}$ in sample 1.

the spin-gap opening above T_c in the Cu(2) NSLRR; the transition shown in Fig. 3(a) is even sharper than in other NMR results, since our measurement corresponds to the orientation $H_0 \| a$-b plane. Furthermore, the spin susceptibility, as deduced from the oxygen MHS, never decreases for temperatures larger than T_c (as it does in substoichiometric YBCO), but rather increases with decreasing temperature, a behavior characteristic of the overdoped compounds.[34] Regarding the properties of sample 1, we also note that the width of the superconducting transition ($\cong 2$ K) is rather large as compared to the best $YBa_2Cu_3O_7$ (0.3 K). This should be regarded as a consequence of Sr impurities, and not as a sign of an inhomogeneity of oxygen concentration: this latter would induce a distribution of the MHS, and thus a temperature dependence of the O(2,3) NMR linewidths, which is not observed. Finally, in our data analysis we used the inelastic neutron-scattering measurements by Rossat-Mignod and co-workers[24,25] which were also carried out on a $YBa_2Cu_3O_{6+x}$ single crystal grown in the same place along the same procedure as ours,[30] and also made of barium with 3.5% strontium impurities (4% in our sample 1). All the neutron measurements have been carried out on one big crystal in which the oxygen concentration x has been varied to cover the whole phase diagram. These results were confirmed by other groups supposedly working on pure YBCO,[26,35] at least for $x < 0.9$ where other results are available. Note that the NMR data for sample 2, which is really Sr free and belongs to the 60-K plateau, must be compared to the neutron data obtained by Rossat-Mignod *et al.*[24,25] for $x = 0.69$ ($T_c = 59$ K) and *not* for $x = 0.52$ (the presence of strontium limits the ordering of oxygen vacancies in the CuO chains and makes T_c substantially lower). In any case, we analyzed the NMR and neutron data taken in the equivalent samples and the analysis is thus fully self-consistent, even if it turns out that the effect of Sr impurities in $x = 1$ samples are somehow important.

Measurements were performed with fixed external magnetic field $H_0 = 5.75$ T using a modified CXP-100 spectrometer and a Nicolet LAS12/70 for data acquisition, both being monitored by a PC. In the NSLRR measurements, the following modification of the standard π-t-$\pi/2$-τ-π pulse sequence was used:

$\pi_{(-y)}$-t-	$\pi/2_{(x)}$-τ-$\pi_{(y)}$	sign of data acquisition:	+
-t-	$\pi/2_{(x)}$-τ-$\pi_{(y)}$	sign of data acquisition:	−
$\pi_{(y)}$ -t-	$\pi/2_{(x)}$-τ-$\pi_{(y)}$	sign of data acquisition:	+
-t-	$\pi/2_{(x)}$-τ-$\pi_{(y)}$	sign of data acquisition:	−,

which eliminates unwanted stray stimulated echo signals and provides directly the difference between signals at time t and infinity. In this case, relaxation rate is determined just by a two-parameter fit to the theoretical curve,[33] which increases the precision and reliability of results. For the O(2,3) site, the data were obtained on the first low-frequency satellite, and results were occasionally checked on the second low-frequency satellite as discussed in Ref. 8.

In the comparison of the a and b components of oxygen MHS reported here to the ones obtained from oriented powder samples, one should note that in the latter case the value is determined from the position of "van Hove" singularity of the "two-dimensional" powder spectrum, while in the case of a single crystal MHS corresponds to the line peak as illustrated in Fig. 4. Naturally, the precision of single-crystal data is much better.[33]

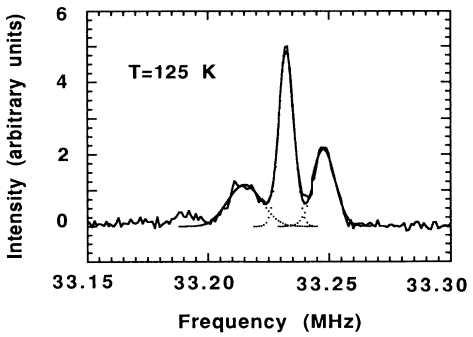

FIG. 4. Line shape corresponding to the $(-1/2, 1/2)$ transition in sample 2 for O(2,3) and O(4) nuclei and the orientation $H_0 \| a$ and b axis. These two spectra are superposed due to the twinning of the single crystal along (110). The solid line corresponds to a computer fit with a Gaussian line shape. The fit of the O(4) line shape (the low-frequency line) is only provisional, since two distinct transitions are fitted with only one Gaussian.

III. RESULTS

The EFG tensors experienced by the nuclei at the O(2) and O(3) sites has been determined by fitting the line position of the complete spectrum (i.e., five lines for each site) for the orientation $H_0 \| c$ axis.[28] The largest component of the tensor V_{ZZ} is along the Cu—O—Cu bond, and the smallest one V_{XX} along the c axis, thus defining a local coordinate system at the planar oxygen sites shown in Fig. 5. Knowing the EFG parameters, which are found to be temperature independent, one can easily determine the complete MHS tensors as a function of the temperature—using just the line positions of central lines, as shown in Fig. 4. Note that (Fig. 5) when H_0 is perpendicular to the c axis and parallel to the a axis [b axis] of the crystal, H_0 is along the Z axis (i.e., parallel to the Cu—O—Cu bond) for site O(2) [O(3)], and along the Y axis (i.e., perpendicular to the Cu—O—Cu bond) for site O(3) [O(2)]. Because the crystals are twinned along (110), when H_0 is oriented parallel to the a axis (and perpendicular to the c axis) in one type of domain, it is automatically parallel to the b axis in the other type of domain, leading to the spectrum, which is a superposition of lines corresponding to both O(2) and O(3) sites and both $H_0 \| Y$ and $H_0 \| Z$ orientations. The EFG tensors of two sites are only slightly different so that customarily, for each orientation Z, Y, and $c = X$, we speak of the O(2,3) line which may be split in two as shown in Fig. 2(a). No significant difference could be detected in the corresponding MHS and NSLRR tensors. (In order to detect the possible difference in NSLRR, the analysis of relaxation has been occasionally performed on the Fourier transform of the echo, for two peaks separately.)

Figure 6 summarizes the ^{17}O(2,3) MHS results in sample 1. Note that $K_{\alpha\alpha}$ is slightly increasing when decreasing temperature, which means that the spin susceptibility is not flat, but slightly increasing as already noticed by Walstedt *et al.*[19] by copper and Balakrishnan *et al.*[18] by yttrium MHS. This is now recognized as a signature of overdoped samples,[34] which is the case of pure $YBa_2Cu_3O_7$. Going further in the details, it can be seen that when H_0 is parallel to the c axis, the spin susceptibility seems to pass through a maximum around $T = 110$ K, whereas when H_0 is in the a-b plane there is definitely no decrease of MHS down to T_c.

Figure 7 shows the temperature dependence of all the components of the O(2,3) NSLRR tensor; the most important feature of these data is that $(^{17}T_1T)^{-1}$ also continuously increases when decreasing the temperature

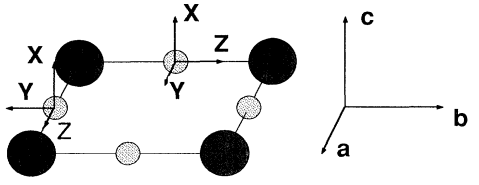

FIG. 5. Principal axes of the electric-field-gradient tensor at O(2) and O(3) sites.

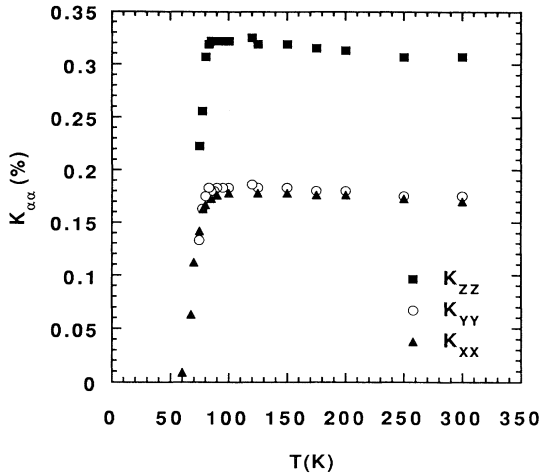

FIG. 6. Principal components (Fig. 5) of the MHS tensor for O(2,3) sites in sample 1 ($YBa_{1.92}Sr_{0.08}Cu_3O_7$ single crystal).

from 350 K down to T_c, although this increase is much less pronounced than that for the Cu(2) $(^{63}T_1T)^{-1}$. However, the increase is clearly stronger than the one observed by the MHS and it is more pronounced when H_0 is in the a-b plane (the same is true for the MHS). Note that in $YBa_2Cu_3O_7$ only a temperature independent behavior (Fig. 8) has been reported so far[7,14] corresponding to the c-axis component of NSLRR measured on oriented powders. One possible explanation is that in these cases the increasing behavior has been hidden by experimental error, relatively limited temperature range, and by the fact that in these samples one actually observes a small "precursor decrease" of NSLRR somewhat above T_c—which flattens out the $(T_1T)^{-1}$ vs T dependence (Fig. 8). Another possibility is that these data came from slightly substoichiometric samples, where constant $(T_1T)^{-1}$ corresponds to MHS (i.e., static suscepti-

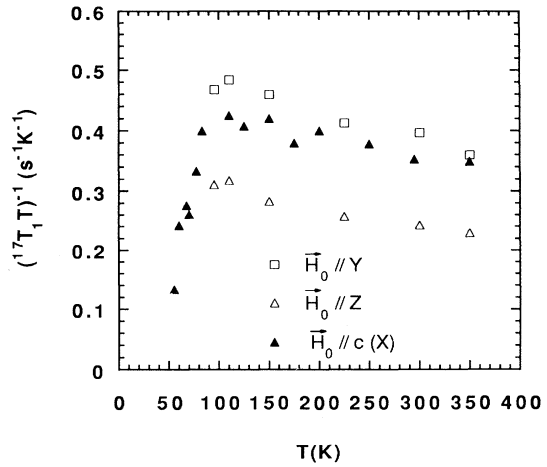

FIG. 7. Principal components (Fig. 5) of the $(T_1T)^{-1}$ tensor for O(2,3) sites in sample 1.

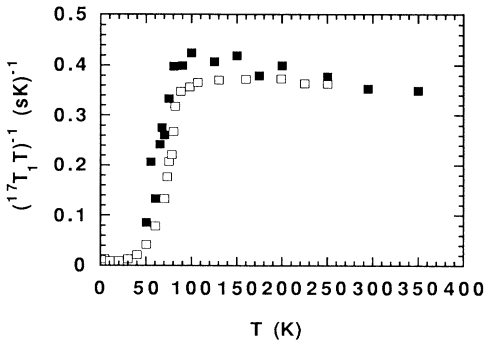

FIG. 8. The $(T_1T)^{-1}$ for O(2,3) sites with H_0 parallel to the c axis in sample 1 (■) compared to oriented powder data (□) reported in Ref. 7.

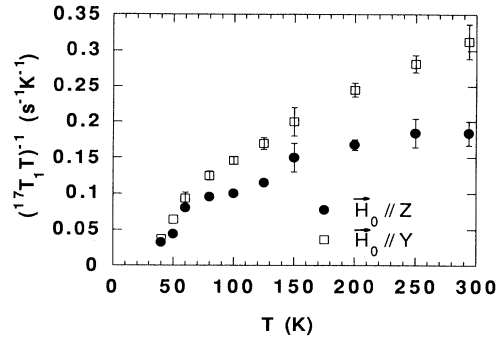

FIG. 10. The in-plane components (Fig. 5) of $(T_1T)^{-1}$ tensor for O(2,3) sites in sample 2. Note a slight change in the slope at $T=T_c$.

bility) which is slightly decreasing with temperature, so that the ratio $(T_1T)^{-1}/K$ presents the same temperature dependence as in sample 1.

The MHS and $(T_1T)^{-1}$ of sample 2 shown in Figs. 9 and 10 show strong temperature dependence of these quantities, which is essentially equal (or equivalent—note the difference in samples and technique) to those already reported in 60-K-phase samples.[9,14,29] As we see in Fig. 11, the relationship between K_{ZZ} and K_{YY} is linear (the slope $\Delta K_{ZZ}/\Delta K_{YY}=1.7\pm0.02$) even in the superconducting regime, and the lowest values $K_{ZZ}=0.06\pm0.005$ and $K_{YY}=0.02\pm0.005$ (measured at 30 K) are just between those determined by Takigawa *et al.*[9] and Yoshinari *et al.*[14] As in the case of $H_0\|c$-axis data,[9,14] in Fig. 12 we see that the $(T_1T)^{-1}$ for the $H_0\|Y$ axis is found to be accurately proportional to the MHS, while $H_0\|Z$ data reveal deviations from this behavior below 100 K (and perhaps also above 250 K). A very important consequence is that the anisotropy of the relaxation rate $R_{YZ}=(T_{1Y}T)^{-1}/(T_{1Z}T)^{-1}$ is temperature dependent (Fig. 13) as already observed by Barriquand *et al.*[29] We have checked that the decrease of the NSLRR anisotropy measured in sample 2 below ~100 K (a value of $R_{YZ}=1.17$ is found at 60 K) is not an artifact of the cross relaxation between the oxygen nuclei in the $H_0\|Z$- and

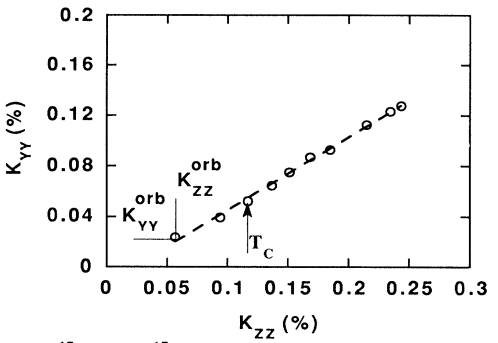

FIG. 11. $^{17}K_{ZZ}$ vs $^{17}K_{YY}$ with the temperature as an implicit parameter (sample 2); note that the linear relationship still holds below T_c.

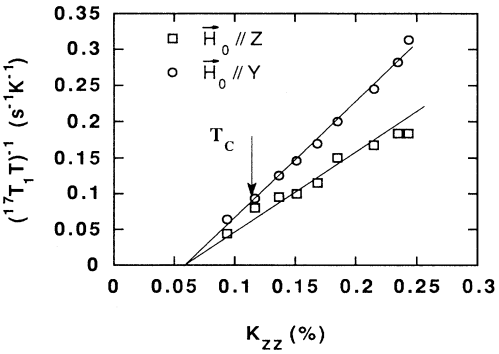

FIG. 12. $(T_{1_Z}T)^{-1}$ and $(T_{1_Y}T)^{-1}$ plotted as a function of K_{ZZ} for sample 2.

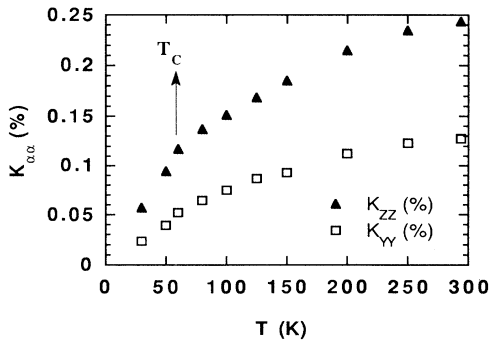

FIG. 9. The in-plane components (Fig. 5) of MHS tensor for O(2,3) sites in sample 2 ($YBa_2Cu_3O_{6.52}$ single crystal).

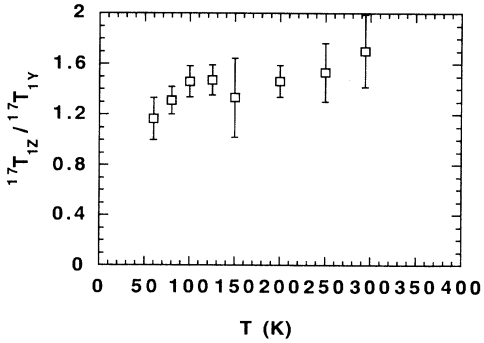

FIG. 13. Temperature dependence of NSLRR anisotropy T_{1_Z}/T_{1_Y} in sample 2.

$H_0 \| Y$-axis configurations (these oxygen nuclei are the nearest neighbors), which may proceed via the $(1/2, -1/2)$ transition, as these NMR lines overlap for temperature just above T_c. Our cross-relaxation experiment showed that this effect cannot significantly influence the results of the NSLRR measurements.

Returning to the discussion of the proportionality between $(T_{1_Y}T)^{-1}$ and MHS data, we note that the extrapolation of this dependence, i.e., of

$$K_{ZZ(YY)}(T)=\alpha(T_{1Y}T)^{-1}+K_{ZZ(YY)}(0)\ , \tag{1}$$

to $T=0$ leads to the values $K_{ZZ(YY)}(0)$ which are the *same* as those directly measured at 30 K. This point is actually very important as it confirms the *precise* proportionality between $(T_{1Y}T)^{-1}$ and the spin part of MHS, $K^{\rm spin}=K(T)-K(T=0)$. Note that for small deviations from proportionality we would still observe linear relation (1) (within the given precision of experimental data), however, the so-deduced $K_{ZZ(YY)}(0)$ values would be smaller or greater than zero-temperature MHS, corresponding to $(Y_{1Y}T)^{-1}$ decreasing with temperature slower or faster than the MHS.

Let us now consider the temperature dependence of the ratio of copper and oxygen NSLRR $^{63/17}R=(^{63}T_1/^{17}T_1)^{-1}$ shown in Fig. 14. Our results in the normal state of sample 1 ($YBa_{1.92}Sr_{0.08}Cu_3O_7$) show that $^{63/17}R$ is continuously increasing when decreasing T from 300 K down to T_c. It was first claimed by Hammel *et al.*[7] that $^{63/17}R$ in $YBa_2Cu_3O_7$ was increasing when decreasing the temperature from room temperature down to 120 K and then kept constant. More recently, Yoshinari *et al.*[36] have repeated these measurements and found that $^{63/17}R$ was increasing when decreasing from room temperature down to 100 K, flattens between 100 and 77 K (with $T_c=87$ K) and then decreases down to the room temperature value when decreasing further the temperature. However, in their samples, both $(^{63}T_1T)^{-1}$ and $(^{17}T_1T)^{-1}$ start to decrease well above T_c, which seems to indicate that their sample is actually slightly substoichiometric. We think that the behavior observed on our sample 1 is the correct one when there is no opening of any gap in the AF spin fluctuations, a situation corresponding to a true overdoped compound.

If we now turn to the 60-K phase, we see that $^{63/17}R$ in sample 2 shows a pronounced flattening starting below T^*, the temperature corresponding to the maximum of $(^{63}T_1T)^{-1}$ when decreasing temperature from 300 K down to T_c. This differs from the behavior reported by Takigawa *et al.*[9] in $YBa_2Cu_3O_{6.63}$ where $^{63/17}R$ was found continuously increasing down to T_c; however, we believe that our result, reflecting the opening of the pseudogap for magnetic excitations, is typical for underdoped samples, which is corroborated by the same behavior observed in $YBa_2Cu_4O_8$ by Zheng *et al.*[37]

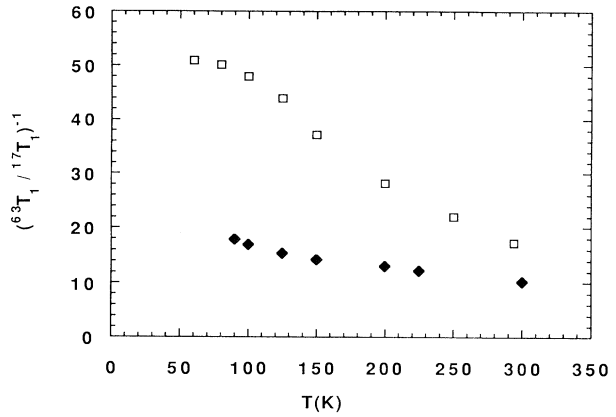

FIG. 14. Temperature dependence of copper to oxygen NSLRR ratio (with $H_0 \| c$ axis) in samples 1 (♦) and 2 (□). For sample 1 the copper $^{63}T_{1_c}$ data were actually simulated by the $(3.4\times{}^{63}T_{1_{a,b}})$ data, i.e., by the $^{63}T_{1_{a,b}}$ corrected for the corresponding NSLRR anisotropy.

IV. DISCUSSION

The key point in the interpretation of the data is of course the choice of the Hamiltonian connecting the nuclear spins (i.e., the NMR probe) and the (electronic) system under investigation. Namely, all the formulas used in the interpretation of the MHS and NSLRR are actually precisely defined by this Hamiltonian. We shall limit the discussion to the so-called Mila-Rice Hamiltonian,[6] which seems to be quite successful in describing the NMR data, and which was recently also corroborated by the microscopic derivation.[23] The principal assumption is that, as far as the nuclear spins are concerned, there is only *one relevant variable* in the system, namely, the electronic spin **S** localized at the Cu(2) sites. Each nuclear spin is supposed to be linearly coupled to the nearest-neighboring (NN) copper spins **S**, so that for ^{63}Cu(2), ^{17}O(2,3) nuclei in the CuO_2 plane, and nearby ^{89}Y, the Hamiltonian equals

$$H=\sum_i\left[{}^{63}\gamma\hbar\,{}^{63}\mathbf{I}_i\cdot\mathbf{A}\cdot\mathbf{S}_i+{}^{63}\gamma\hbar\sum_{\delta=1}^{4}B\,{}^{63}\mathbf{I}_i\cdot\mathbf{S}_{i+\delta}+{}^{17}\gamma\hbar\sum_{\delta'=1}^{2}{}^{17}\mathbf{I}_i\cdot\mathbf{C}\cdot\mathbf{S}_{i+\delta'}+{}^{89}\gamma\hbar\sum_{\delta''=1}^{8}{}^{89}\mathbf{I}_i\cdot\mathbf{D}\cdot\mathbf{S}_{i+\delta''}\right]\ , \tag{2}$$

where A is the Cu(2) on-site hyperfine coupling tensor, and B is the hyperfine coupling constant at the Cu(2) site transferred from the four NN Cu(2) spins (which is assumed to be a scalar corresponding to the coupling realized via an on-site s orbital), C is the hyperfine coupling tensor at the O(2,3) site transferred from each of its two NN Cu(2) spins, and D is the hyperfine coupling tensor at the Y site transferred from each of its eight NN Cu(2)

spins via the oxygen orbitals.

Note that *a priori* we have to admit the possibility of the existence of an independent oxygen $2p$ band whose interaction with oxygen (or yttrium) nuclei cannot be represented by (i.e., reduced to) coupling to Cu(2) spins **S**. As this possibility is *not* taken into account in the Mila-Rice Hamiltonian, we start the following paragraph by the precise formulation of the analysis of the oxygen MHS tensor data,[5] used to prove the neglect of an independent oxygen contribution in the Hamiltonian (2).

A. Magnetic hyperfine shift

Experimentally, the MHS tensor of planar oxygen has a nearly axial symmetry with respect to the Z axis (Fig. 5), and it is convenient to decompose its spin part $^{17}\mathbf{K}^{\rm spin}$ into the isotropic ($K_{\rm iso}$) and axial ($K_{\rm ax}$) components as follows:

$$K^{\rm spin}(\theta)=K_{\rm iso}+K_{\rm ax}(3\cos^2\theta-1)/2 \ , \tag{3}$$

where θ is the angle between the external applied magnetic field H_0 and the Z axis. Taking into account both the contribution transferred from NN copper and the contribution of an oxygen p band, one can write:[5]

$$K^{\rm spin}_{\rm iso}=(2f_s A_{2s}/g\mu_B)\chi^{\rm spin}_{\rm Cu} \ , \tag{4a}$$

$$K^{\rm spin}_{\rm ax}=(2f_p A_{2p}/g\mu_B)\chi^{\rm spin}_{\rm Cu}+(A_{2p}/g\mu_B)\chi^{\rm spin}_{\rm holes} \ , \tag{4b}$$

where A_{2p} (A_{2s}) are the hyperfine coupling constants associated to an unpaired spin in the oxygen $2p$ ($2s$) orbitals, and f_p (f_s) are the fraction (per Cu) of oxygen $2p$ ($2s$) orbitals polarized by overlap and hybridization with Cu $3d$ orbitals. Below T_c, both $\chi^{\rm spin}_{\rm Cu}$ as well as $\chi^{\rm spin}_{\rm holes}$ vanish, and at $T=0$ the MHS is reduced to its orbital component $K_{\rm ax}(T=0)=K^{\rm orb}_{\rm ax}$ and $K_{\rm iso}(T=0)=K^{\rm orb}_{\rm iso}$, which is expected and supposed to be temperature independent. In the normal state, if there is no contribution from the oxygen band, i.e., if $\chi^{\rm spin}_{\rm holes}=0$, both $K^{\rm spin}_{\rm ax}$ and $K^{\rm spin}_{\rm iso}$ components will be proportional to $\chi^{\rm spin}_{\rm Cu}$; in the 60-K-phase samples, using the strong temperature dependence of MHS, we will then experimentally verify that two components are precisely proportional. Conversely, any deviation from proportionality will indicate the presence of $\chi^{\rm spin}_{\rm holes}$ (which is then distinguished from $\chi^{\rm spin}_{\rm Cu}$ by different temperature dependence).

Using an argument equivalent to the one exposed in the preceding section in the discussion of proportionality between $(T_{1_Y}T)^{-1}$ and MHS, we see that the essential point in this test is the precise determination of orbital (i.e., $T=0$) MHS. The proportionality is actually verified, and from Eq. (4b) we see that this means that the magnitude of the term $(A_{2p}/g\mu_B)\chi^{\rm spin}_{\rm holes}$ is smaller or equal to the error bars on $K^{\rm ax}_{\rm orb}$. In our measurements, we can estimate this error to 0.006%, which corresponds to the upper limit for $\chi_{\rm holes}$ equal to 2×10^{-6} e.m.u./mole of O(2,3).

In the following, we will suppose that $\chi_{\rm holes}=0$ and, consequently, that Mila-Rice Hamiltonian (2) provides a full description of the system. Putting $f_s A_{2s}=C_{\rm iso}$ and $f_p A_{2p}=C_{\rm ax}$ in Eq. (4) we obtain the equation

$$^{17}K^{\rm spin}_{\alpha\alpha}=2C_{\alpha\alpha}\chi^{\rm spin}_{\rm Cu}/g\mu_B \ , \quad \alpha=X,Y,Z \ , \tag{5}$$

which directly corresponds to the oxygen part of the Mila-Rice Hamiltonian (2). Using the temperature dependence of the susceptibility and MHS, from Eq. (5) one can deduce the hyperfine coupling tensor C. This was not possible in our case, as the susceptibility data were polluted due to a small amount of "green phase" hard to avoid in the type of crystal we have used. We thus refer the reader to the values given by Yoshinari *et al.*,[14] who also found that $C_{\alpha\alpha}$ values are rather independent of the composition. (This result relies on the assumption that the total spin susceptibility χ^S (expressed in e.m.u./mole) is equally distributed over Cu(2) and Cu(1) sites, i.e., that $\chi^{\rm spin}_{\rm Cu}=\chi^S/[(2+x)N_A]$, where N_A is the Avogadro number—a hypothesis, which remains to be proved.) Taking their values, $C_{ZZ}=157$ kOe, $C_{YY}=90$ kOe, and $C_{XX}=96$ kOe, we found that in $YBa_{1.92}Sr_{0.08}Cu_3O_7$ (sample 1) the χ^S increases from 0.90×10^{-4} to 0.96×10^{-4} e.m.u./mole of Cu, when the temperature decreases from 300 to 120 K; Graf and coworkers[34] showed that such an increase of $\chi^S(T)$ vs decreasing temperature is a characteristic of the overdoped YBCO.

In $YBa_2Cu_3O_{6.52}$, χ^S decreases from 0.66×10^{-4} to 0.20×10^{-4} e.m.u./mole of Cu when the temperature decreases from 300 to 60 K. The microscopic origin of the decrease of the static spin susceptibility, which seems to be systematically related to the appearance of the opening above T_c of a pseudogap for the antiferromagnetic excitations (directly observed by neutron or NMR in $La_{1-x}Sr_xCuO_4$, $YBa_2Cu_4O_8$, and substoichiometric YBCO) is one of the theoretical challenges offered by the high-T_c superconductors at the moment. Recently, such a decrease of χ^S has been obtained by quantum dynamical Monte Carlo calculations[38] and also in the analysis of the t-J model given by Tanamoto, Kohno, and Fukuyama,[39] however, experimentally, the AFF are at the same time increasing with decreasing temperature, contrary to the corresponding theoretical prediction of the t-J model.

B. Nuclear spin-lattice relaxation

From the Mila-Rice Hamiltonian, the NSLRR of nuclei can be expressed as

$$(^nT_1T)^{-1}=k_B(\gamma_n^2/2\mu_B^2)\sum_{\mathbf{q}}|^nA_{\alpha\alpha}(\mathbf{q})|^2\chi''(\mathbf{q},\omega_n)/\omega_n \ , \tag{6}$$

where index n denotes the chosen nucleus (^{63}Cu, ^{17}O, or ^{89}Y), and $\chi''(\mathbf{q},\omega_n)$ is the imaginary part of magnetic susceptibility of localized copper spins **S** (in **q** space, at the NMR frequency $\omega_n\cong0$). Taking into account the relative position of nucleus and NN copper spins, we obtain the following form factors, i.e., the Fourier-transformed hyperfine coupling constants (squared):

$$|^{63}A_{\parallel}(\mathbf{q})|^2=[A_{\perp}+2B(\cos q_a a+\cos q_b b)]^2 \quad \text{for } H_0\|c \text{ axis}, \tag{7a}$$

$$|^{63}A_{\perp}(\mathbf{q})|^2=1/2\{[A_{\perp}+2B(\cos q_a a+\cos q_b b)]^2+[A_{\parallel}+2B(\cos q_a a+\cos q_b b)]^2\} \quad \text{for } H_0\perp c \text{ axis}, \tag{7b}$$

$$|^{17}A_{\gamma\gamma}(\mathbf{q})|^2=(C_{\alpha\alpha}^2+C_{\beta\beta}^2)[1+(\cos q_a a+\cos q_b b)/2] \tag{7c}$$

and

$$|^{89}A_{\gamma\gamma}(\mathbf{q})|^2=4(D_{\alpha\alpha}^2+D_{\beta\beta}^2)(1+\cos q_a a)(1+\cos q_b b)(1+\cos q_z c) \quad \text{for } H_0\|\gamma \text{ axis}, \tag{7d}$$

where α,β,γ correspond to any circular permutation of the local directions X,Y,Z defined in Fig. 5. The presence of antiferromagnetic fluctuations means that $\chi''(\mathbf{q},\omega_n)$ is peaked at the antiferromagnetic wave vector $\mathbf{Q}_{AF}=(\pi/a,\pi/a)$. If the AF peak of χ'' is strong, this contribution will be dominant in the ^{63}Cu relaxation where $^{63}A(\mathbf{Q}_{AF})\neq 0$, however, it will be strongly suppressed (filtered out) in oxygen and yttrium relaxation as $^{17,89}A(\mathbf{Q}_{AF})=0$, and for these nuclei relaxation is determined by the contribution around $\mathbf{q}=\mathbf{0}$. Experimentally, the difference in the magnitude and the temperature dependence of $(^{63}T_1T)^{-1}$ and $(^{17}T_1T)^{-1}$ has been the first evidence for the existence of AFF in the normal phase of $YBa_2Cu_3O_{6+x}$.[7] This is now definitively confirmed by the inelastic neutron scattering, which provides the direct measurement of $\chi''(\mathbf{q},\omega)$ as a function of both variables.[24–26]

In the following, we will try to put together coherently the NMR NSLRR data interpreted within the above-exposed formalism and the neutron data, in order to obtain maximum information on $\chi''(\mathbf{q},\omega)$. Note that neutrons provide information corresponding to energies of a few meV or greater, while for NMR $\hbar\omega_n$ is four to five orders of magnitude smaller. In order to compare the data, we describe $\chi''(\omega)$ measured by neutrons by a Lorentzian,

$$\chi''(\omega)=\chi(0)\frac{\omega\Gamma(\omega)/\pi}{[\Gamma(\omega)/\pi]^2+\omega^2}, \tag{8}$$

in which we allow for an energy dependence of Γ. For $\Gamma(\omega_{max})/\pi=\omega_{max}$ this function attains its maximum $\chi''_{max}=\chi''(\omega_{max})=\chi(0)/2$. As the neutron data provide $\chi''(\omega)$ in arbitrary units, it is convenient to normalize them by the maximum value; in this way $\chi(0)$ is eliminated from Eq. (8) and $\chi''(\omega)/\chi''_{max}$ can be directly transformed to the energy dependent Γ. From the neutron results,[24–26,35] which are available for $\mathbf{Q}_{AF}$, and for samples with $T_c\geq 60$ K, we find that $\hbar\Gamma(\mathbf{Q}_{AF},\omega_{max})/\pi$ equals 25–30 meV and is essentially independent of temperature and sample composition. Below $\sim$15 meV the $\chi''(\mathbf{Q}_{AF},\omega)$ is proportional to ω, and the corresponding $\Gamma(\mathbf{Q}_{AF},\omega\sim 0)$ is 2–3 times greater. [As an aside we remark that, within the present description, an opening of the gap or pseudogap[40] with decreasing temperature is reflected as an anomalous increase of $\Gamma(\omega\sim 0)$.] We assume that this proportionality holds down to the NMR frequency, so that, from the zero frequency limit of Eq. (8), for NMR we obtain the relation,

$$\frac{\chi''(\mathbf{q},\omega_n)}{\omega_n}=\frac{\chi(\mathbf{q},\omega=0)}{\Gamma(\mathbf{q},\omega=0)/\pi}, \tag{9}$$

connecting $(T_1T)^{-1}$ [via Eqs. (6) and (7)] and the MHS [via Eq. (5)] to the characteristic energy Γ. Independently of Eq. (8), we can always regard Eq. (9) as the definition of Γ measured by NMR. Equation (8) enables us to compare energy scales measured by neutrons and NMR, if we accept that the description given by Eq. (8) is meaningful.

Neutron results[24–26,35] also provide us information on $\mathbf{q}$ dependence of χ'' near $\mathbf{Q}_{AF}$. While the *shape* of the AF peak as a function of $\mathbf{q}$ is not precisely resolved, we know that its full width at half maximum $\Delta q/[2^{1/2}2\pi/a]$ is temperature independent and equal to 0.124 and 0.27 for 60-K and 90-K phase samples, respectively. Moreover, the energy dependence of Δq is negligible at 5–20 meV, and we will assume that the same is valid down to the NMR frequency, i.e., in our analysis of NMR data, we take Δq fixed to the above given values as the principal parameter taken over from neutron data.

In the analysis of NMR data we first deduce hyperfine coupling tensors and static susceptibility $\chi(\mathbf{q}=\mathbf{0},\omega=0)$ from the MHS measurements [Eq. (5)]. Then, we assume a particular functional form for the AF peak of χ'', try to adjust the magnitude of AF enhancement $\chi''(\mathbf{Q}_{AF})/\chi''(0)$ and see if we can consistently fit the temperature dependence of the normal state NSLRR for all the nuclei. If in the fit we find unsolvable incompatibility of various data, we should doubt the validity of starting (model) Mila-Rice Hamiltonian. Successful fit would confirm the Mila-Rice description and supply us with the full and detailed information on $\mathbf{q}$ and temperature dependence of magnetic susceptibility.

We remark that, throughout this section we will consider only the relaxation rates measured in the c-axis direction, corresponding to the in-plane fluctuations of magnetic field. In this way the analysis does not depend on the anisotropy of spin susceptibility, if it exists. The anisotropy of relaxation is thus treated separately: for copper Cu(2) as an additional (and optional) constraint on the choice of the copper coupling constants, while for the oxygen it is discussed in detail in Sec. V. Unfortunately, in our 60-K phase single crystal the oxygen $^{17}T_{1_{c=X}}$ data are not available and we replaced them with $^{17}T_{1_Y}$ values, which are nearly the same due to the symmetry with respect to the Z axis (Fig. 5). The temperature dependence of the anisotropy of oxygen relaxation, discussed in Sec. V, is driven only by $^{17}T_{1_Z}$ data; it is natural to ex-

pect that any additional (anomalous) contribution to relaxation first shows up in the Z axis data, as the relaxation is much slower in this direction.

The central point in the analysis of NMR data is that the anomalous temperature dependence of AFF [measured by Cu $(T_1T)^{-1}$] is suppressed by the oxygen (and yttrium) form factor and does not affect oxygen NSLRR. We thus begin by looking at oxygen data to see quantitatively how efficient this filtering is, and from Eqs. (5), (6), (7c), and (9) we deduce the following formula:

$$\Gamma(\mathbf{q}=\mathbf{0},\ \omega=0)=\left[\frac{\pi\,{}^{17}\gamma^2 k_B}{2\mu_B}(C_{ZZ}^2+C_{XX}^2)^{1/2}\right]\left[\frac{(K_{ZZ}^2+K_{XX}^2)^{1/2}}{({}^{17}T_{1_Y}T)^{-1}}\right],$$
$$\times\left[\sum_q\{1+(\cos q_a a+\cos q_b b)/2\}\frac{\chi''(\mathbf{q},\omega_n)}{\chi''(\mathbf{0},\omega_n)}\right], \tag{10}$$

which proved to be very convenient. Note that in 60-K phase strong temperature variations of $({}^{17}T_{1_{c,Y}}T)^{-1}$ and MHS are precisely proportional (see Fig. 12 for the $H_0\|Y$ data in our sample 2 and Refs. 9 and 14 for the corresponding $c=X$ data), making the second bracket of Eq. (10) constant, while in the overdoped sample 1 this term is only weakly temperature dependent. The third bracket measures the efficiency of the AFF filtering by the oxygen form factor; for perfect filtering it should be equal to 1, while the deviation from perfect filtering would increase this number and at the same time make it temperature dependent—it will increase with decreasing temperature reflecting the anomalous temperature dependence of copper $({}^{63}T_1T)^{-1}$. The crucial point in our analysis of oxygen data is that, having in mind formula (1), we *interpret* the precise proportionality of $({}^{17}T_{1_{c,Y}}T)^{-1}$ and MHS in the 60-K phase as the *proof* that the filtering *is* perfect and that $\Gamma(\mathbf{q}=\mathbf{0})$ is temperature independent. Another possibility is that the temperature dependence of the third bracket of Eq. (10) (induced by imperfect filtering) is *by chance* equal to the temperature dependence of $\Gamma(\mathbf{q}=\mathbf{0})$, as supposed by Monien *et al.*[22,23] Note that there is *no* physical reason for these two different quantities, corresponding to different excitations ($\mathbf{q}=\mathbf{0}$ and $\mathbf{Q}_{AF}$) with completely different temperature dependences, to be proportional. Moreover, if we allowed for the unknown temperature dependence of $\Gamma(\mathbf{q}=\mathbf{0})$ in the fit, we would actually introduce an *arbitrary function,* which can "explain" any difference between temperature dependences of copper and oxygen relaxation whatever the $\mathbf{q}$ dependence of χ'' is, and this would make the fit essentially useless for the moment. The only possibility to experimentally verify the hypothesis of perfect filtering is to perform precise measurements of the temperature dependence of the ratio of oxygen to yttrium NSLRR ${}^{17/89}R$ in the *same* sample (one should be able to discern the ${}^{17/89}R(T)$ variations of less than $\sim 5\%$). Namely, due to the different form factors (7c) and (7d) the filtering is significantly more efficient at Y than at O(2,3), and any remaining AFF component in oxygen relaxation would show up in the temperature dependence of ${}^{17/89}R$. Unfortunately, these data are not yet available.

In the following we will consider that in the 60-K phase the filtering is perfect, which will immediately allow us [from Eq. (10)] to obtain the precise value of $\hbar\Gamma(\mathbf{q}=\mathbf{0})=0.26$ eV. This value is significantly greater than $\Gamma(\mathbf{Q}_{AF})$ measured by neutrons (if we allow for imperfect filtering, it can increase up to 0.30–0.36 eV, in accord with Ref. 22), so that in the further analysis, for the sake of generality, we allow for the $\mathbf{q}$ dependence of Γ.

It is interesting to note that $\Gamma(\mathbf{0})$ does not vary much with the oxygen concentration; if we suppose that in our overdoped sample 1 the filtering of AFF is also perfect, we arrive at a value $\hbar\Gamma(\mathbf{q}=\mathbf{0})=0.30$ eV. Taking into account the corrections of AFF, to be discussed below, this value is actually not smaller than 0.35 eV and strongly depends on the type of the fit. In order to interpret this quantity [let us remember that in an ordinary metal $\hbar\Gamma(\mathbf{q}=\mathbf{0})=N(E_F)^{-1}$] it is worthwhile to go back to another formulation of Eq. (6), i.e., to

$$1/T_1\propto\sum_{\mathbf{q}}|{}^{17}A(\mathbf{q})|^2\int\langle S_{\mathbf{q}}(t)S_{-\mathbf{q}}(0)\rangle e^{i\omega_n t}dt \tag{11a}$$
$$\propto\sum_{\mathbf{q}}|{}^{17}A(\mathbf{q})|^2\langle S_{\mathbf{q}}(0)S_{-\mathbf{q}}(0)\rangle\tau_c \tag{11b}$$
$$\propto\langle|S_{\mathbf{q}\cong\mathbf{0}}(0)|^2\rangle\tau_c\ , \tag{11c}$$

where Eq. (11b) formally defines correlation time τ_c, while Eq. (11c) is valid only approximately, since the oxygen form factor is peaked at $\mathbf{q}=\mathbf{0}$. Again, $\hbar/\tau_c$ represents the energy width of the spectral weight of the excitations, and the perfect filtering constraint tells us that the mean square amplitude of the spin fluctuations around $\mathbf{q}=\mathbf{0}$ and the static spin susceptibility are proportional. Since both of them have to be proportional to the number of unpaired spin in the system, we may suspect that this number of unpaired spin is the physical quantity, which varies with temperature in substoichiometric YBCO.

The simplest way to take into account the $\mathbf{q}$ dependence of Γ is to divide the χ'' into $\mathbf{q}$ independent part and AF enhanced part, i.e., to replace Eq. (9) by

$$\frac{\chi''(\mathbf{q},\omega_n)}{\omega_n}=\frac{\chi(\mathbf{0})}{\Gamma(\mathbf{0})/\pi}+\Phi(\mathbf{q}-\mathbf{Q}_{AF})\frac{\chi(\mathbf{Q}_{AF})}{\Gamma(\mathbf{Q}_{AF})/\pi}\ , \tag{12}$$

where all the q dependence of χ'' is absorbed in the

shape-function Φ satisfying $\Phi(\mathbf{0})=1$ and $\Phi(|\mathbf{Q}_{\rm AF}|)\cong 0$. From Eq. (12), it is clear that the AF enhancement is measured by

$$\frac{\chi''(\mathbf{Q}_{\rm AF},\omega_n)}{\chi''(\mathbf{0},\omega_n)}=1+\frac{\chi(\mathbf{Q}_{\rm AF})/\Gamma(\mathbf{Q}_{\rm AF})}{\chi(\mathbf{0})/\Gamma(\mathbf{0})} . \tag{13}$$

The left-hand side of Eq. (13) and the $\Gamma(\mathbf{0})$ are the quantities, which are deduced from the NMR relaxation data analysis, so that the $\Gamma(\mathbf{Q}_{\rm AF})$ value determined by neutrons is only necessary if one wants to deduce $\chi(\mathbf{Q}_{\rm AF})/\chi(\mathbf{0})$ ratio.

Before proceeding with the data analysis, we have to complete two more steps: (i) to assume a certain shape for the AF enhancement $\Phi(\mathbf{q}-\mathbf{Q}_{\rm AF})$, and verify whether we can indeed obtain the perfect AFF filtering, and (ii) to choose the values of the copper hyperfine coupling tensors A and B (for oxygen we stick to C values[14] mentioned in the preceding section).

Three possibilities have been taken into consideration for the $\mathbf{q}$ dependence of the AF enhancement of χ'':

(1) squared Lorentzian $\Phi_L(\mathbf{q})=1/(1+\xi^2 q^2)^2$. (14a)

(2) Gaussian $\Phi_G(\mathbf{q})=\exp(-\ln 2\xi^2 q^2)$, (14b)

and

(3) "four Gaussians" $\Phi_{4G}(\mathbf{q})=\frac{1}{4}\sum_{i=1}^{4}\exp(-\ln 2\xi^2[q-\mathbf{Q}^i_{\rm AF}]^2)$ (14c)

centered at four incommensurate positions near $\mathbf{Q}_{\rm AF}$, i.e., at $\mathbf{Q}^i_{\rm AF}/(2\pi/a)$ equal to $(1/2\pm\delta,1/2)$ and $(1/2,1/2\pm\delta)$, with $\delta=0.07$, as proposed by Tranquada *et al.* to explain the $\mathbf{q}$ dependence of $\chi''(\mathbf{q},\omega)$ of their neutron data in $YBa_2Cu_3O_{6.5}$.[35] The only parameter in the shape functions, i.e., ξ/a is determined so that the full width at half maximum (FWHM) of the AFF peak of χ'' matches the value measured by neutron scattering. For $\Phi_L(\mathbf{q})$ and $\Phi_G(\mathbf{q})$ we can find that ξ/a equals $(2^{1/2}-1)^{1/2}/(2^{1/2}\pi\Delta q)$ and $1/(2^{1/2}\pi\Delta q)$, respectively, where Δq is expressed in relative lattice units (i.e., in units of $2^{1/2}2\pi/a$ for the scan along the diagonal in two-dimensional $\mathbf{q}$ space). For the case of $\Phi_{4G}(\mathbf{q})$, by fitting the original neutron data from Ref. 35 we obtained $\xi/a=3.3$.

Note that $\Phi_L(\mathbf{q})$ has been chosen to simulate the same shape for χ'' as originally proposed by MMP;[21,23] however, the formulation is different. Originally, motivated by the RPA approximation, MMP actually proposed that

$$\chi(\mathbf{q})=\frac{\chi_0(T)\beta^{1/2}(\xi/a)^2}{1+\xi^2(\mathbf{Q}_{\rm AF}-\mathbf{q})^2}$$

and (15)

$$\Gamma(\mathbf{q})=\frac{\Gamma[1+\xi^2(\mathbf{Q}_{\rm AF}-\mathbf{q})^2]}{\beta^{1/2}(\xi/a)^2} .$$

However, the $\Gamma(\mathbf{Q}_{\rm AF})$, which is then deduced from the NMR data is an order of magnitude smaller than the value measured by neutrons, so that using Eq. (15) we see no way to make an interpretation consistent with neutron data.

The Gaussian shapes correspond to the minimization of the total $\mathbf{q}$ width of the AFF, which in turn provides the most efficient filtering of AFF by the oxygen form factor. With respect to this, we can regard the four hardly separated Gaussian $\Phi_{4G}(\mathbf{q})$, proposed by Tranquada *et al.*[35] as the shape having the steepest sides. However, the interpretation where the position of the incommensurate peaks is determined by nesting of the Fermi surface[35] is not straightforward because the same position is used for La-Ba-Sr-Cu-O and YBCO, while the corresponding Fermi surfaces are rotated by 45°.[41]

The choice of the copper hyperfine coupling tensors A and B is much more difficult than for oxygen because the temperature dependence of $^{63}K_{cc}$ and $^{63}K_{ab}$ corresponds to $A_\parallel+4B$ and $A_\perp+4B$, leaving one unknown parameter. This parameter is then deduced either using the value of the local magnetic field in the Néel phase of $YBa_2Cu_3O_6$ (assuming that the coupling constants have not changed), or from the fit to the experimental value of the anisotropy of copper relaxation. In the latter case, from Eqs. (6), (7a), and (7b) it is easy to see that when AFF peak dominates copper relaxation,

$$(^{63}T_{1_\perp}/^{63}T_{1_\parallel})^{-1}\cong\frac{|^{63}A_\perp(\mathbf{Q}_{\rm AF})|^2}{|^{63}A_\parallel(\mathbf{Q}_{\rm AF})|^2}=\frac{1}{2}\left[\frac{(A_\parallel-4B)^2}{(A_\perp-4B)^2}+1\right] . \tag{16}$$

Some deviations from Eq. (16) are expected for finite strength and q width of the AFF, inducing also the weak temperature dependence for the predicted NSLRR an-

TABLE I. The ^{63}Cu coupling constants used in the fit: (a) as given in the analysis of Shimizu *et al.* (Ref. 12) and (b), while $(A_\parallel+4B)$ and $(A_\perp+4B)$ were constrained to values deduced from ^{63}Cu MHS data by Shimizu *et al.* (Ref. 12) the transferred coupling B was adjusted so that the fitted value of copper NSLRR anisotropy be in accord with the experiment.

	60 K		90 K	
	(a)	(b)	(a)	(b)
$A_\parallel$ (kOe)	−344	−359	−440	−510
$A_\perp$ (kOe)	8	20	24	−46
B (kOe)	91.5	79	93	107

isotropy. Coupling constants derived from both procedures agree fairly well, however, the results of the fit are rather sensitive to even small variations of the coupling constants. In our analysis we thus used two sets of coupling constants given in Table I, which are both deduced from the work of Shimizu *et al.*[12] (The values for the 60-K phase are not significantly different from those obtained by Takigawa *et al.*[9])

As already mentioned, the central point in the analysis of oxygen relaxation is to determine the degree of filtering of AFF. Precise measure of this quantity is given by the ratio between the experimental value of $(^{17}T_{1_{c,Y}}T)^{-1}$, and the one computed by taking into account only the AF contribution [i.e., putting in Eq. (12) $\chi(\mathbf{0})=0$], a quantity we call $(^{17}T_{1_{AF}}T)^{-1}$. As long as copper relaxation is dominated by the AF contribution, this ratio is equal to the ratio between the calculated value $^{63/17}R_{AF}=(^{63}T_{1_{AF}}T)^{-1}/(^{17}T_{1_{AF}}T)^{-1}$ and the experimental value $^{63/17}R_{exp}$. (Here we only multiplied previously mentioned quantities by the copper $(^{63}R_1T)^{-1}$, in order to eliminate all the unknown parameters except for the shape function Φ, and thus simplify the calculation of $^{63/17}R_{AF}$.) The values of $^{63/17}R_{AF}$ calculated for the 60-K phase and Φ_L, Φ_G, and Φ_{4G} shapes of AFF given by Eqs. (14a), (14b), and (14c) are 31, 115, and 162, respectively. Compared to the experimental values shown in Fig. 14 [$^{63/17}R_{exp}(150\text{K})=37$], we see that even the narrowest four-Gaussian shape can hardly satisfy the condition of efficient filtering of AFF. While Gaussian shape provides only somewhat less efficient filtering, any other shape function Φ decreasing slower than the Gaussian (e.g., Φ_L) is definitely ruled out.

For Φ_G and Φ_{4G} functions, more details on the complete fit corresponding to our two samples and two characteristic temperatures are given in Table II. The table is organized to follow the fit procedure, which was chosen to be as simple as possible. The χ_0 was calculated directly from the oxygen MHS and the corresponding coupling constants,[14] so that this value is considered "experimental" (it is not a fit parameter). First, for a high-temperature point, the experimental values of $^{17}T_{1_{c,Y}}$ and $^{63}T_{1_c}$ were fitted to define $\Gamma(0)$ and the AF-enhancement coefficient $\chi(\mathbf{Q}_{AF})\Gamma(0)/\chi(0)\Gamma(\mathbf{Q}_{AF})$. Then, for a low-temperature point, $^{63}T_1$ is fitted to define AF-enhancement coefficient at this temperature, from the fit we read $^{17}T_1$ and compare it with the experimental value—a mismatch not greater than 10% might be considered tolerable for the given temperature variation of input (experimental) data. As already mentioned above, the fit is found to be strongly dependent on ^{63}Cu coupling constants. To show the corresponding variations of fit parameters, two different sets of coupling constants (given in Table I) were used for each type of fit. The values are taken to be as reported in Ref. 12 (in agreement with Ref. 9), and we did *not* optimize the values within the generous experimental error to improve the fit. As an important result of the fit, in Table II we also included the $(T_{1_{AF}}/T_1)^{-1}$ parameter measuring the AFF contribution to the relaxation.

Fit prediction of low temperature $(^{17}T_{1_{c,Y}}T)^{-1}$ is always found to be somewhat too high, indicating that the filtering of AFF is not sufficient, as already predicted from the discussion of $^{63/17}R$ values given above. Note that $\Gamma(\mathbf{q}=\mathbf{0})$ is assumed to be temperature independent, and the enhancement of AFF with respect to the $\mathbf{q}=\mathbf{0}$ susceptibility will always produce an overestimate in the fit over the $(^{17}T_1T)^{-1}\propto K$ behavior, the question is only whether this effect is negligible or not. The overestimate depends on the shape and the q width of the AFF (e.g., in

TABLE II. Fit of the ^{63}Cu(2) and ^{17}O(2,3) NSLRR in $YBa_2Cu_3O_{6+x}$, using the (I) "four Gaussians" (14c) and (II) Gaussian (14b) shape of the AF enhancement of χ'' (the shape parameters ξ/α and δ were deduced from the neutron scattering data). The T_1 data correspond to $H_0\|c$ axis; only for ^{17}O in 60-K sample this value is replaced by nearly the same Y-axis value. Different ^{63}Cu coupling constants used in the fit are given in Table I. Fit parameters and details of the fit procedure are explained in the text.

		60-K sample					90-K sample				
		(Ia)	(Ib)	(IIa)	(IIb)	T(K)	(Ia)	(Ib)	(IIa)	(IIb)	T(K)
Expt.	χ_0 (10^{-4} emu)		0.62					0.90			
	$(^{63}T_1T)^{-1}$ ($s^{-1}K^{-1}$)		6.2					4.0			
	$(^{17}T_1T)^{-1}$ ($s^{-1}K^{-1}$)		0.277					0.355			
Fit	$\Gamma(\mathbf{q}=\mathbf{0})$ (eV)	0.30	0.32	0.32	0.36	250	0.50	0.35	0.81	0.39	300
	$\chi(\mathbf{Q}_{AF})\Gamma(0)/\chi(0)\Gamma(\mathbf{Q}_{AF})$	160	267	54	94		44	11	26	4.2	
	$(^{63}T_{1\perp}/^{63}T_{1/\!/})^{-1}$	2.7	3.4	2.7	3.4		4.4	3.4	4.6	3.4	
Expt.	χ_0 (10^{-4} emu)		0.45					0.96			
	$(^{63}T_1T)^{-1}$ ($s^{-1}K^{-1}$)		7.4					7.0			
Fit	$\chi(\mathbf{Q}_{AF})\Gamma(0)/\chi(0)\Gamma(\mathbf{Q}_{AF})$	281	457	94	160		79	23	44	8.6	
Expt.	$(^{17}T_1T)^{-1}$ ($s^{-1}K^{-1}$)		0.20			150		0.43			100
Fit results	$(^{17}T_{1fit}/^{17}T_{1exp.})^{-1}$	1.10	1.15	1.13	1.20		1.17	1.02	1.30	1.08	
	$(^{63}T_{1AF}/^{63}T_1)^{-1}$	0.85	0.89	0.85	0.90	250	0.78	0.57	0.86	0.61	300
	$(^{17}T_{1AF}/^{17}T_1)^{-1}$	0.12	0.18	0.17	0.26		0.40	0.14	0.63	0.22	
	$(^{63}T_{1AF}/^{63}T_1)^{-1}$	0.90	0.93	0.91	0.94	150	0.87	0.74	0.92	0.76	100
	$(^{17}T_{1AF}/^{17}T_{1fit})^{-1}$	0.19	0.28	0.26	0.38		0.55	0.26	0.75	0.36	

our fit of 60-K data the overestimate is reduced by a factor of 2 when the q width is decreased by 30%) and on the values of the coupling constants (e.g., compare the corresponding columns a and b in Table II). For the q width given by the INS data, we can see that, depending on the values of the ^{63}Cu coupling constants, this overestimate can be reduced below 10%, i.e., to the tolerable level. In the 60-K data the efficient filtering is actually very demanding because $(^{17}T_{1_{c,Y}}T)^{-1}$ strongly decreases with decreasing temperature, while the AF contribution to it [measured by $(^{63}T_1T)^{-1}$] is increasing somewhat. This causes the relative AF contribution $(T_{1_{AF}}/T_1)^{-1}$ to increase strongly and to show up in the fit at low temperature. We did not fit the 60-K data below 150 K, where the pseudogap starts to open,[40] since the simple extrapolation of INS data to "zero-frequency" NMR values is no longer possible in this case.

Note that, experimentally, perfect filtering holds down to T_c (Fig. 12), which can happen, for example, in the following scenario. We suppose that the opening of the spin gap, i.e., the loss in the spectral weight in the low-energy part of $\chi''(\mathbf{q},\omega)$, does not take place uniformly in $\mathbf{q}$ space. The temperature dependence of the O(2,3) NSLRR can be interpreted as the signature of the opening of the gap for the excitations around $\mathbf{q}=\mathbf{0}$, which has already started at room temperature. On the other hand, the opening of the pseudogap concerning the AFF around $\mathbf{Q}_{AF}$ starts to be effective only below $T^*\approx 150$ K; above T^*, there is no sign of redistribution of the spectral weight in $\chi''(\mathbf{q},\omega)$ from the neutron data obtained for samples with $T_c\cong 60$ K. It is thus reasonable to think that for the intermediate values of $\mathbf{q}$, the opening of the gap takes place at an intermediate temperature, which is greater than T^*. Due to oxygen form factor (7c), the contribution of the AFF to the NSLRR of O(2,3) site is mainly due to this intermediate $\mathbf{q}$ range. As soon as the pseudogap starts to open (at frequencies close to zero) at these values of $\mathbf{q}$, the corresponding AFF contribution to the oxygen spin-lattice relaxation will be immediately suppressed, while nothing has been observed yet by neutrons (i.e., at higher energies). Such a picture strongly differs from the one given by Monien and co-workers,[21–23] where the whole dynamic spin susceptibility is factored by the static susceptibility $\chi'(\mathbf{q}=\mathbf{0})$ and the temperature dependence of $\chi'(\mathbf{q}=\mathbf{0})$ determines opening of a spin gap uniformly in $\mathbf{q}$ space. Our different point of view is supported by recent neutron[42] experiments in Zn-doped YBCO, showing that the spin gap at $\mathbf{Q}_{AF}$ can be completely suppressed without any modification of the temperature dependence of the spin susceptibility $\chi'(\mathbf{q}=\mathbf{0})$ as seen by yttrium NMR.[43]

Finally, the experimentally perfect filtering might also indicate the existence of some other mechanism different from our model based on the Mila-Rice Hamiltonian. This possibility is corroborated by the oxygen NSLRR anisotropy data, which cannot be explained within this model, which is discussed in Sec. V.

In the overdoped sample, the AF enhancement is much wider in $\mathbf{q}$ space, and the fit gives at least 20% of increase of $(^{17}T_1T)^{-1}$ as temperature is lowered from 300 to 100 K, as observed in our sample 1. In this case, it is definitely *not* possible to obtain the efficient filtering within our model, i.e., it is not possible to fit the oxygen NSLRR with $^{17}(T_1T)^{-1}$ and $\chi(\mathbf{q}=\mathbf{0})$, which are both temperature independent. This reassures our assumption that the oxygen relaxation measured in our sample 1 (Fig. 7) gives the true characteristic of the overdoped YBCO, while previously reported $(^{17}T_{1_c}T)^{-1}=\text{const}$[7,14] data correspond to substoichiometric samples, as already mentioned in Sec. III. Conversely, if these data were true, there have to be effects that are not taken into account in our description. As already detailed in the discussion of the 60-K phase data using Eq. (10), we did *not* consider the possibility that the ill-filtered AFF contribution to oxygen relaxation is exactly compensated by the temperature dependence of Γ. In contrast to the original MMP model,[21–23] we assume that Γ is temperature independent, as suggested by the precise proportionality of $(^{17}T_{1_{c,Y}}T)^{-1}$ and MHS in the 60-K phase.

In the analysis of oxygen data in an overdoped sample, it is very important to know whether, once we subtract the temperature dependence due to AFF, the so-obtained $\mathbf{q}=\mathbf{0}$ contribution to $(^{17}T_{1_{c,Y}}T)^{-1}$ is still proportional to the $K(T)$, as it is in the 60-K sample. Unfortunately, due to the uncertainty in the corrections deduced from the fit, for the given very weak temperature dependence of these quantities, we cannot conclude on their relation. In $^{17}[T_{1_{c,Y}}(\mathbf{q}=\mathbf{0})T]^{-1}\propto K(T)^{\alpha}$, we cannot really distinguish between $\alpha=1$ and some other exponent. Of course, the $\alpha=2$ case is very interesting as it corresponds to the true Korringa behavior, and it is consistent with theoretical predictions[39,44,45] that in the overdoped regime we should encounter the Fermi-liquid behavior. Actually, any increase of the α value would indicate the change of the regime, as we should expect $\alpha=2$ only under additional special circumstances, as discussed in Ref. 40. However, from the fit (Table II) we can only say that values $\alpha>1$ are less probable than $\alpha\leq 1$ values. As already mentioned before, one way to improve our knowledge on this point is to perform precise NSLRR measurements on yttrium and oxygen in the same sample. The difference in the corresponding form factors (filtering is more efficient at yttrium) should be clearly "visible" in the NSLRR, as in overdoped samples the $\mathbf{q}$ width of the AFF is very large.

V. ANISOTROPY OF NSLRR

In this section, we shall concentrate on the temperature dependence of the NSLRR for the O(2,3) site. Table III summarizes the oxygen NSLRR anisotropy of samples 1 and 2. While in the 90-K-phase data shown in Fig. 7 the anisotropy is found to be temperature independent, this is definitely not true for the 60-K phase. However, even for sample 2 we found that between 100 and 250 K the anisotropy is approximately constant, as can be seen in Figs. 12 and 13. The value declared in Table III corresponds to this temperature interval.

In the interpretation of these data we first consider the above-defined model, in which the only source of relaxa-

TABLE III. Experimental and calculated [Eq. (17)] NSLRR anisotropy of plane oxygen in the 90-K phase and 60-K phase of YBCO single crystals.

Sample	Ratio	R (expt.)	R (calc.)
	R_{ZX}	0.69±0.05	0.61
1	R_{YX}	1.12±0.10	1.09
	R_{YZ}	1.62±0.15	1.80
2	R_{YZ}	1.47±0.15	1.89

tion of O(2,3) is the fluctuations of neighboring copper spins and the interaction is given by the Mila-Rice Hamiltonian (2) with no other contributions. From Eqs. (6) and (7c), under the assumption that the imaginary part of the copper magnetic susceptibility χ'' is isotropic, we find that the anisotropy of relaxation,

$$R_{\gamma\alpha}=(T_{1\gamma}/T_{1\alpha})^{-1}=(C_{\alpha\alpha}^2+C_{\beta\beta}^2)/(C_{\beta\beta}^2+C_{\gamma\gamma}^2)\ , \tag{17}$$

is completely determined by the static coupling constants only. These have been rather precisely determined from the MHS, and in Table III the experimental anisotropy is also compared to the prediction of Eq. (17), using the coupling constants measured by Yoshinari *et al.*[14] (the ratio C_{ZZ}/C_{YY} agrees with the value 1.7±0.02, which we have precisely determined). While an acceptable agreement is found in sample 1, for sample 2 the difference is considerably greater than the experimental error.

We tried to account for the difference between the calculated and the experimental values by some anisotropy of copper spin susceptibility. If such an anisotropy is present, the real coupling constants determined from MHS are

$$C_{\alpha\alpha}^{\text{real}}=C_{\alpha\alpha}^{\text{exp}}\Delta\chi^{\text{exp}}/\Delta\chi_{\alpha\alpha} \tag{18}$$

and Eq. (17) is replaced by

$$R_{YZ}=\frac{C_{ZZ}^2/C_{YY}^2+rC_{XX}^2/C_{YY}^2}{1+rC_{XX}^2/C_{YY}^2} \quad \text{and} \tag{19a}$$

$$R_{YX}=\frac{C_{ZZ}^2/C_{YY}^2+rC_{XX}^2/C_{YY}^2}{1+C_{ZZ}^2/C_{YY}^2} \tag{19b}$$

where

$$r=\frac{\Delta\chi_{ab}^2}{\Delta\chi_{cc}^2}\frac{\sum_{\mathbf{q}} f(\mathbf{q})\chi_{cc}''(\mathbf{q},\omega_n)}{\sum_{\mathbf{q}} f(\mathbf{q})\chi_{ab}''(\mathbf{q},\omega_n)}\ ,$$
$$f(\mathbf{q})=1+(\cos q_a a+\cos q_b b)/2 \tag{20}$$

is the only unknown factor which measures the susceptibility anisotropy (without anisotropy $r=1$). In order to explain the experimental value of the NSLRR anisotropy in sample 1, a relatively small correction of $r\simeq 1.3$ is enough, which can be accepted as a minor correction to the above discussed model. In $YBa_2Cu_3O_{6.52}$ very strong susceptibility anisotropy $r>2$ has to be invoked, which would clearly demand complete revision of our fit to account consistently for the copper NSLRR data as well. Even if it were possible to do that within our framework of a one-component model, within this model it is *a priori* not possible to have temperature dependent R_{YZ} [i.e., $r=r(T)$] and temperature independent R_{YX} (i.e., $r=$const) at the same time, as seems to be required by the experimental data. Note, however, that for the temperature independence of R_{YX} there are no direct measurements on the same sample; we only know that both T_{1_X} and T_{1_Y} are proportional to the total susceptibility $\chi(T)$.

We remark that, up to now, we have treated the copper electronic spins as localized, and we have implicitly considered that the isotropic and axial components of hyperfine fields (C_{iso} and C_{ax}) due to the polarization of the $2s$ and $2p$ oxygen orbitals were coherent. That is, in our analysis we simply used total Cartesian components of hyperfine coupling tensor. Note that Barriquand, Odier, and Jerome[29] have claimed that s and p contributions add incoherently because the average over the Fermi surface of $C_{\text{iso}}(\mathbf{k})C_{\text{ax}}(\mathbf{k})$ is equal to zero; they invoked symmetry arguments similar to those used by Yafet and Jaccarino to explain how the core-polarization relaxation rate is incoherent with relaxation due to the s band in transition metals.[46] We do not believe this type of argument can apply here, since in the tetragonal symmetry of the problem, all the admixture of $2p$ and $2s$ wave functions with the $d_{x^2-y^2}$ should belong to the same representation Γ_3'. Moreover, one should keep in mind that the polarization of the $2p$ and $2s$ orbitals involves not only the lowest Hubbard band, but also the empty upper one.

To explain the temperature dependence of R_{YZ}, Barriquand, Odier, and Jerome[29] propose that a new mechanism, the motion of Zhang and Rice singlets, brings a contribution, which is growing with the temperature. In spite of the interest of this approach, it is again hard to imagine that both contributions will adjust at all temperatures to give $(T_{1_X}T)^{-1}$ and $(T_{1_Y}T)^{-1}$ proportional to $\chi^S(T)$.

We are thus led to think that the basic contributions to $(^{17}T_1T)^{-1}$ are proportional to $\chi^S(T)$ whatever the direction of the magnetic field X, Y, or Z, but an extra contribution occurs when H_0 is parallel to the Cu—O—Cu bond (Z direction). To explain this additional contribution, we investigate the relaxation associated to an ordinary p-band metal, generalizing the result given by Obata[47] for cubic symmetry to the case of tetragonal symmetry. From the general analysis given in the Appendix, we learn that for pure $|p_Z\rangle$ orbital there is only a dipolar contribution to relaxation, and the Z direction relaxation is 2/5 of the relaxation in the perpendicular direction. When $|p_X\rangle$ and $|p_Y\rangle$ orbitals are admixed, the orbital relaxation comes in as well; however, the ratio of Z-to-perpendicular-direction relaxation (R_{ZX}) is never greater than 1.2 (or even somewhat smaller, if the core-polarization contribution is taken into account). To fit the experimental data we would like to have a contribution that is dominant in the Z direction and negligible (within the experimental error) perpendicular to it. The anisotropy of this kind can be obtained if we suppose that

there is no dipolar relaxation and consider the orbital relaxation only; for small admixtures of $|p_X\rangle$ and $|p_Y\rangle$ orbitals, R_{ZX} would then be close to 2, which is just enough for the extra contribution to relaxation to be coherent with the experiment. Note that pure orbital relaxation corresponds to *spinless holes*, so that this analysis might be evidence of the presence of the holons. However, due to insufficient precision, the data are not conclusive.

In addition to the above-discussed contributions covered by the theory of Obata[47] and Narath,[48] Lee and Nagaosa[49] discussed the relaxation due to the long-range orbital currents in compounds with metallic two-dimensional layers, which might be applicable to the copper-oxide superconductors above T_c. However, the anisotropy of the corresponding contribution is given by $T_{1_a}^{-1}=T_{1_b}^{-1}=1.5T_{1_c}^{-1}$, i.e., there is no difference between the two in-plane directions: parallel (Z) and perpendicular (Y) to Cu—O—Cu bond, while for the out-of-plane direction ($c=X$) the relaxation is faster. Therefore, it is obvious that this mechanism cannot be taken neither as the principal source of the oxygen relaxation where $T_{1_c}^{-1}\cong T_{1_Y}^{-1}\cong 1.5T_{1_Z}^{-1}$, nor as an additional component satisfying $T_{1_Z}^{-1}\gg T_{1_Y}^{-1}$, $T_{1_c}^{-1}$, like the "normal" orbital contribution discussed in the previous paragraph.

VI. CONCLUSION

The comparison between the temperature dependence of Cu(2) and O(2,3) NSLRR in the whole metallic range of $YBa_2Cu_3O_{6+x}$ has given the first evidence for the existence of AFF of copper spins, which are filtered at the oxygen site. This has now been confirmed by inelastic neutron scattering experiments, which in addition have shown that for energies lower than 20 meV, the $\mathbf{q}$ width of $\chi''(\mathbf{q},\omega)$ is energy and temperature independent, while the characteristic energy for the fluctuations is of the order 20–30 meV. At this stage, high quality ^{17}O NMR data including the NSLRR anisotropy become of fundamental importance, as they enable us to perform *quantitative* analysis of the NMR data taking into account the neutron results. Putting these two together provides an accurate way to distinguish between "true" and "false" descriptions of the system. In this article we present MHS and NSLRR data taken in ^{17}O-enriched YBCO single crystals for two different characteristic oxygen concentrations corresponding to the underdoped 60-K phase ($YBa_2Cu_3O_{6.52}$) and the overdoped 90-K phase ($YBa_{1.92}Sr_{0.08}Cu_3O_7$). Since most of the interpretation is based on the Mila-Rice spin Hamiltonian, we reexamine in detail the validity of neglecting the possible existence of a second (oxygen) degree of freedom in the system. As far as the MHS analysis is concerned, one spin degree of freedom is in fact enough to explain the data. In contrast, the temperature dependence of the O(2,3) NSLRR anisotropy *cannot* be explained within the framework of the Mila-Rice Hamiltonian.

In previous work[21–23] the analysis of NMR data leads to the ξ values, which are directly compatible with the INS results only in the special limiting case, which was not discussed in detail.[23] We explore in more detail the possibility of providing a compatible description; the main idea was to take the INS results [ξ inferred from Δq and an estimate of $\Gamma(Q_{AF})$] as a starting point in the analysis of NMR data in order to obtain *a priori* consistent and complete information on q and temperature dependence of χ'', i.e., of the AFF. The Δq, i.e., the width in q space of the AF enhancement of χ'' measured by neutrons, is thus considered to hold for energies as low as the nuclear Larmor frequency. As regards the NMR, this reduces the number of unknown (fit) parameters and permits more decisive conclusions. It turns out that the experimental values Δq are rather large, so that the contribution of the AFF to the O(2,3) NSLRR cannot be easily filtered out by the oxygen form factor. In order to fit the experimental data we are thus forced to use the $\mathbf{q}$ dependence of the AFF that is the most localized around Q_{AF}, i.e., that falls off as fast as possible. We conclude that only a Gaussian (as in Ref. 23), or rather a sum of four slightly incommensurate Gaussians (as a shape having steeper sides), provide a reasonable fit. However, even in these cases the experimental data seem to require more efficient filtering than that provided by the fit. Although the difference is not clearly significant if we take into account the experimental error in the copper coupling constants used in the fit, it suggests that the opening of the spin gap, which is observed in the 60-K phase is nonuniform in $\mathbf{q}$ space.

In the analysis we also discussed in detail the $(^{17}T_{1_{c,Y}}T)^{-1}\propto K(T)$ law, which is valid within the present experimental precision in the 60-K phase. From this we deduce an energy scale for the $\mathbf{q}=\mathbf{0}$ fluctuations that is significantly larger than that for the AFF (determined by the inelastic neutron scattering). As regards the $(^{17}T_{1_{c,Y}}T)^{-1}\propto K(T)$ law, we are unfortunately unable to tell whether the same or some other law is valid in the overdoped samples, since the $\mathbf{q}=\mathbf{0}$ contribution to oxygen relaxation is "polluted" by incompletely filtered AFF. The solution of this question is very interesting with respect to the phase diagram predicted in the framework of the spin-charge separation. We also remark that our overdoped $(^{17}T_1T)^{-1}$ data (Fig. 7) provide the first experimental evidence of insufficient filtering of the AFF and it is important to verify this behavior on other samples. All the other data we obtained on single crystals are in accord with data (mostly in oriented powders) already reported by other groups.[7,9,12,14]

Finally, in our analysis of the AFF we tried to use only the c-axis NSLRR data, which correspond to the in-plane fluctuations only. (In the absence of $^{17}T_{1_{c=X}}$ data, in our 60-K phase single crystal we used $^{17}T_{1_Y}$ values, which are almost the same, owing to the symmetry with respect to the Z axis parallel to the Cu—O—Cu bond.) In this way we avoided the problems of possible anisotropy of χ''. If this existed, it would change only the discussion of the NSLRR anisotropy. Indeed, the anisotropy of ^{17}O NSLRR (revealed by $^{17}T_{1_Z}$ data) shows that the Mila-Rice Hamiltonian cannot account for the data in the 60-K phase. We also tried to introduce into the analysis the correction which comes from the anisotropy of suscepti-

bility: however, it turns out that any single-component description is unlikely to account for the observed temperature dependence of the anisotropy. The simplest way out was to suppose that corrections are due to an additional degree of freedom associated with an oxygen band. As an interesting consequence, we find that these corrections in NSLRR can be explained in the metallic-band picture, only if they originate from spinless particles (which provide only orbital contribution to relaxation). The available precision of experimental data does not allow a quantitative description, and further experiments are needed in order to clear up this interesting hypothesis.

ACKNOWLEDGMENTS

This work was supported by the Direction des Recherches et des Etudes Techniques (DRET Contract No. 89/045) and by the Ministère de la Recherche et de la Technologie (MRT Contract No. 90.A.0579). One of us (M.H.) would like to acknowledge the support of the EEC Project No. CI1*0568. Laboratoire de Spectrométrie Physique is Unité Associée au CNRS No. 8.

APPENDIX: NSLRR OF AN ORTHORHOMBIC p-BAND METAL IN THE TIGHT-BINDING APPROXIMATION

Following closely the procedure of Obata[47] and Narath,[48] we calculate the dipole and the orbital contribution to the NSLRR of a p-wave electronic band made of $|p_X\rangle$, $|p_Y\rangle$, and $|p_Z\rangle$ orbitals with respective weights C_X, C_Y, and C_Z ($C_X+C_Y+C_Z=1$) corresponding to the orthorhombic symmetry:

$$T_1^{-1}=(4\pi/\hbar)(\hbar\gamma_n)^2 k_B T[\rho_\sigma(E_F)]^2 H_{\rm orb}^2 a \ , \tag{A1}$$

where $H_{\rm orb}=(\hbar\gamma_e)\langle r^{-3}\rangle$ is the orbital hyperfine field, $a=a^{\rm dip}+a^{\rm orb}$ is the geometrical factor to be calculated in the tight-binding approximation, and $\rho_\sigma(E_F)$ is the total density of states per spin direction (summed over all the three p bands). When the angular dependence of $|p_\alpha\rangle$ ($\alpha=X,Y,Z$) orbital is simply given by α/R and the magnetic field H_0 is taken to be parallel to the Z axis, for the geometrical factor we obtain

$$\begin{aligned} a^{\rm dip}&=[4C_Z^2+10(C_X^2+C_Y^2)\\ &\quad +9C_Z(C_X+C_Y)+18C_XC_Y]/100 \ ,\\ a^{\rm orb}&=C_Z(C_X+C_Y) \ . \end{aligned} \tag{A2}$$

This result can easily be reduced for the case of the axial (tetragonal) symmetry, for the magnetic field parallel to the symmetry axis

$$C_Z=x \ , \quad C_X=C_Y=(1-x)/2 \ ,$$

and perpendicular to the symmetry axis

$$C_X=x \ , \quad C_Z=C_Y=(1-x)/2 \ ,$$

where x is the weight of the orbital, which is parallel to the symmetry axis. We obtain

$$\begin{aligned} &a_\parallel^{\rm dip}=[19-20x+9x^2]/200 \ , \quad a_\parallel^{\rm orb}=x(1-x) \ ,\\ &a_\perp^{\rm dip}=[23+8x+9x^2]/400 \ , \quad a_\perp^{\rm orb}=(1+x)(1-x)/4 \ . \end{aligned} \tag{A3}$$

Note the special cases of (i) a single p band: $x=1\Rightarrow a^{\rm orb}=0$, $a_\parallel^{\rm dip}=1/25$, $a_\perp^{\rm dip}=1/10$, $a_\perp/a_\parallel=5/2$, and (ii) the cubic symmetry: $x=1/3\Rightarrow a_\parallel=a_\perp=13/45$, $a_\perp/a_\parallel=1$. The x dependence of the geometrical factor a, as well as the anisotropy of the NSLRR $a_\perp/a_\parallel$ is shown in Fig. 15. We note that for most of the x values the anisotropy of the orbital and dipole NSLRR is less than 20%. Particularly on the side of the single p orbital, a very small admixture of perpendicular orbitals will quickly suppress the initially well expressed anisotropy. If only the orbital part of relaxation is taken into account, corresponding to a particle with zero spin, the anisotropy of relaxation is

$$a_\perp^{\rm orb}/a_\parallel^{\rm orb}=(1+x)/(4x) \ , \tag{A4}$$

which is close to 1/2 for small admixtures of orbitals perpendicular to the symmetry axis.

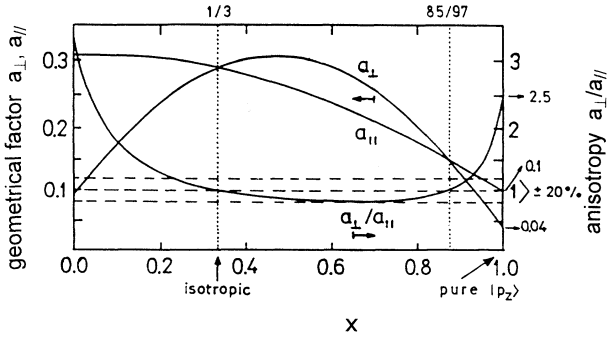

FIG. 15. The NSLRR of a tetragonal p-band metal as a function of the composition of the band. The variables are defined in the text.

*Also at Institute of Physics of the University, P.O.B. 304, 41001 Zagreb, Croatia. Present address: SNCI-CNRS, B.P. 166X, 38042 Grenoble Cedex, France.

†Permanent address: Department of Physics and Solid State Science Center, University of California, Los Angeles, CA 90024.

[1]For a panel, see *Proceedings of the International M^2HTSC Conference,* Lake Kanazawa, 1991 [Physica C **185-9** (1991)].

[2]M. Horvatić, P. Ségransan, C. Berthier, Y. Berthier, P. Butaud, J. Y. Henry, M. Couach, and J. P. Chaminade, Phys. Rev. B **39**, 7332 (1989).

[3]M. Horvatić, P. Butaud, P. Ségransan, Y. Berthier, C. Berthier,

J. Y. Henry, and M. Couach, Physica C **166**, 151 (1990).
[4]C. H. Pennington, D. J. Durand, C. P. Slichter, J. P. Rice, E. D. Bukowski, and D. M. Ginsberg, Phys. Rev. B **39**, 274 (1989); **39**, 2902 (1989).
[5]M. Horvatić, Y. Berthier, P. Butaud, Y. Kitaoka, P. Ségransan, C. Berthier, H. Katayama-Yoshida, Y. Okabe, and T. Takahashi, Physica C **159**, 689 (1989).
[6]F. Mila and T. M. Rice, Physica C **157**, 561 (1989).
[7]P. C. Hammel, M. Takigawa, R. H. Heffner, Z. Fisk, and K. C. Ott, Phys. Rev. Lett. **63**, 1992 (1989).
[8]P. Butaud, M. Horvatić, Y. Berthier, P. Ségransan, Y. Kitaoka, C. Berthier, and H. Katayama-Yoshida, Physica C **166**, 301 (1990); C. Berthier, Y. Berthier, P. Butaud, M. Horvatić, Y. Kitaoka, and P. Ségransan, in *Dynamics of Magnetic Fluctuations in High T_c Materials,* Vol. 246 of *NATO Advanced Study Institute, Series B: Physics,* edited by G. Reiter, P. Horsh, and G. Psaltakis (Plenum, New York, 1990), p. 73.
[9]M. Takigawa, A. P. Reyes, P. C. Hammel, J. D. Tompson, R. H. Heffner, Z. Fisk, and K. C. Ott, Phys. Rev. B **43**, 247 (1991).
[10]E. P. Maarschall, in *Proceedings of the XVIth Congress Ampere, Bucharest, 1970,* edited by I. Ursu (Publishing House of the Academy of Romania, Romania, 1971); C. Bucci and G. Guidi, Phys. Rev. B **9**, 3053 (1974).
[11]P. W. Anderson, in *Frontiers and Borderlines in Many-Particle Physics,* Proceedings of the International School of Physics "Enrico Fermi," Course CIV, Varenna, 1987, edited by R. A. Broglia and J. R. Schrieffer (North-Holland, Amsterdam, 1988).
[12]T. Shimizu, H. Yasuoka, T. Tsuda, K. Koga, and Y. Ueda, Bull. Mag. Res. **12**, 39 (1990).
[13]Y. Kitaoka, Y. Berthier, P. Butaud, M. Horvatić, P. Ségransan, C. Berthier, H. Katayama-Yoshida, Y. Okabe, and T. Takahashi, Physica C **162-4**, 265 (1990).
[14]Y. Yoshinari, H. Yasuoka, Y. Ueda, K. Koga, and K. Kosuge, J. Phys. Soc. Jpn. **59**, 3698 (1990).
[15]H. Alloul, T. Ohno, and P. Mendels, Phys. Rev. Lett. **63**, 1700 (1989).
[16]M. Horvatić, C. Berthier, Y. Berthier, P. Butaud, W. G. Clark, J. A. Gillet, P. Ségransan, and J. Y. Henry, *Proceedings of the International M^2HTSC Conference,* Ref. 1, p. 1139.
[17]H. Alloul, P. Mendels, H. Casalta, J. F. Marucco, and J. Arabski, J. Less Common Metals **164-5**, 1022 (1990).
[18]G. Balakrishnan, R. Dupree, I. Farnan, D. McK. Paul, and M. E. Smith, J. Phys. C **21**, L847 (1988).
[19]R. E. Walstedt, R. F. Bell, L. F. Schneemeyer, J. V. Waszczak, and G. P. Espinosa, Phys. Rev. B **45**, 8045 (1992).
[20]H. Zimmerman, M. Mali, J. Roos, D. Brinkmann, J. Karpinski, E. Kaldis, and S. Rusiecki, Physica C **159**, 681 (1989); H. Zimmerman, M. Mali, I. Mangelschots, J. Roos, L. Paul, D. Brinkmann, J. Karpinski, S. Rusiecki, and E. Kaldis, J. Less Common Metals **164-5**, 138 (1990); I. Mangelschots, M. Mali, J. Roos, D. Brinkmann, S. Rusiecki, J. Karpinski, and E. Kaldis, Physica C **194**, 277 (1992).
[21]A. J. Millis, H. Monien, and D. Pines, Phys. Rev. B **42**, 167 (1990).
[22]H. Monien, D. Pines, and M. Takigawa, Phys. Rev. B **43**, 258 (1991).
[23]A. J. Millis and H. Monien, Phys. Rev. B **45**, 3059 (1992).
[24]J. Rossat-Mignod, L. P. Regnault, C. Vettier, P. Burlet, J. Y. Henry, and G. Lapertod, Physica B **169**, 58 (1991).
[25]J. Rossat-Mignod, L. P. Regnault, P. Bourges, C. Vettier, P. Burlet, and J. Y. Henry, Phys. Scr. T **45**, 74 (1992); review article by J. Rossat-Mignod, L. P. Regnault, P. Bourges, P. Burlet, C. Vettier, and J. Y. Henry, in *Frontiers in Solid State Sciences: Magnetism and Superconductivity* (World Scientific, Singapore, in press).
[26]P. Bourges, P. M. Gehring, B. Hennion, A. H. Moudden, J. M. Tranquada, G. Shirane, S. Shamoto, and M. Sato, Phys. Rev. B **43**, 8690 (1991).
[27]C. Berthier, Y. Berthier, P. Butaud, W. G. Clark, J. A. Gillet, M. Horvatić, P. Ségransan, and J. Y. Henry, *Proceedings of the International M^2HTSC Conference,* Ref. 1, p. 1141; in *Electronic Properties and Mechanisms of High T_c Superconductors,* edited by T. Oguchi, K. Kadowaki, and T. Sasaki, (Elsevier, Amsterdam, 1992), p. 347.
[28]M. Horvatić, Ph.D. thesis, University of Zagreb, 1991.
[29]F. Barriquand, P. Odier, and D. Jerome, Physica C **177**, 230 (1991).
[30]J. Y. Henry (unpublished).
[31]F. Borsa, A. Rigamonti, M. Corti, J. Ziolo, Ok-Bae Hyun, and D. R. Torgeson, Phys. Rev. Lett. **68**, 698 (1992).
[32]S. E. Barrett, J. A. Martindale, D. J. Durand, C. H. Pennington, C. P. Slichter, T. A. Friedmann, J. P. Rice, and D. M. Ginsberg, Phys. Rev. Lett. **66**, 108 (1991).
[33]M. Horvatić, J. Phys.: Condens. Matter **4**, 5811 (1992).
[34]T. Graf, G. Triscone, and J. Muller, J. Less Common Met. **159**, 349 (1990); J. Y. Genoux, T. Graf, A. Junod, D. Sanchez, G. Triscone, and J. Muller, Physica **177**, 315 (1991).
[35]J. M. Tranquada, P. M. Gehring, G. Shirane, S. Shamoto, and M. Sato, Phys. Rev. B **46**, 5561 (1992).
[36]Y. Yoshinari, H. Yasuoka, and Y. Ueda, J. Phys. Soc. Jpn. **61**, 770 (1992).
[37]G. Zheng, Y. Kitaoka, K. Asayama, Y. Kodoma, and Y. Yamada (unpublished).
[38]G. Dopf, A. Mutsumara, and W. Hanke, Phys. Rev. Lett. **68**, 353 (1992).
[39]T. Tanamoto, H. Kohno, and H. Fukuyama, J. Phys. Soc. Jpn. **61**, 1882 (1992).
[40]M. Horvatić, T. Auler, C. Berthier, Y. Berthier, P. Butaud, W. G. Clark, J. A. Gillet, P. Ségransan, and J. Y. Henry, Phys. Rev. B **47**, 3461 (1993).
[41]R. J. Radtke, S. Ullah, K. Levin, and M. R. Norman, Phys. Rev. B **46**, 11 975 (1992).
[42]K. Kakurai, S. Shamoto, T. Kiyokura, M. Sato, J. M. Tranquada, and G. Shirane, Phys. Rev. B **48**, 3485 (1993).
[43]H. Alloul, P. Mendels, H. Casalta, J. F. Marucco, and J. Arabski, Phys. Rev. Lett. **67**, 3140 (1991).
[44]H. Fukuyama, Y. Hasegawa, and Y. Suzumura, Physica C **153-5**, 1630 (1988); T. Tanamoto, H. Kohno, and H. Fukuyama, J. Phys. Soc. Jpn. **61**, 1886 (1992); **62**, 717 (1993).
[45]N. Nagaosa and P. A. Lee, Phys. Rev. B **45**, 966 (1992).
[46]Y. Yafet and V. Jaccarino, Phys. Rev. **133**, 1630 (1964).
[47]Y. Obata, J. Phys. Soc. Jpn. **18**, 1020 (1963).
[48]A. Narath, Phys. Rev. **162**, 320 (1967).
[49]P. Lee and N. Nagaosa, Phys. Rev. B **43**, 1223 (1991).